

## Electronic Supplementary Information (ESI)

### **Avobenzene Incorporation in a Diverse Range of Ru(II) Scaffolds Produces Potent Potential Antineoplastic Agents**

Raphael T. Ryan,<sup>a</sup> Dmytro Havrylyuk,<sup>a</sup> Kimberly Stevens,<sup>a</sup> L. Henry Moore,<sup>b</sup> Doo Young Kim,<sup>a</sup> Jessica S. Blackburn,<sup>b</sup> David K. Heidary\*,<sup>a</sup> John P. Selegue\*,<sup>a</sup> and Edith C. Glazer\*<sup>a</sup>

<sup>a</sup>Department of Chemistry, University of Kentucky, 505 Rose Street, Lexington, Kentucky 40506, USA.

<sup>b</sup>Department of Molecular and Cellular Biochemistry, University of Kentucky, 741 S. Limestone, Lexington, KY 40536, USA.

Corresponding Authors:

Edith C. Glazer (ec.glazer@uky.edu)

John. P. Selegue (selegue@uky.edu)

David K. Heidary (david.heidary@uky.edu)

## **Contents**

### **1. Materials and instrumentation.**

### **2. HPLC analysis for purity, stability and photoejection products**

Table S1: HPLC gradient used for determination of purity and photoejection products

### **3. Synthesis and characterization of 1–5**

### **4. Counterion exchange**

### **5. Photoejection studies**

Figures S1–S3, Table S2

### **6. Cell culture**

### **7. Cytotoxicity studies**

Figure S4

### **8. Aqueous stability**

### **9. DNA gel electrophoresis**

Figure S5

### **10. Calf Thymus DNA interactions**

### **11. Singlet Oxygen detection**

### **12. Toxicity assays in zebrafish**

### **13. Additional figures**

Figures S6–31

### **14. References**

## 1. Materials and instrumentation

All materials purchased from commercial sources were used without any further purification. Water used for synthesis, purification, and biological studies was obtained from a Milli-Q® purification system. All  $^1\text{H}$  NMR spectra were obtained on a Varian Mercury spectrometer (400 MHz) and chemical shifts are reported relative to the residual solvent peak of  $\text{CD}_3\text{CN}$  ( $\delta$  1.94), acetone- $\text{D}_6$  ( $\delta$  2.05) or  $\text{CD}_3\text{OD}$  ( $\delta$  3.31).  $^{13}\text{C}$  NMR spectra were obtained on either a Bruker Avance NEO (100 MHz) or a JEOL ECZr spectrometer (125 MHz) with chemical shifts referenced to residual solvent peaks of  $\text{CD}_3\text{CN}$  ( $\delta$  1.32),  $\text{CDCl}_3$  ( $\delta$  77.16) or acetone- $\text{d}_6$  ( $\delta$  29.84). Electrospray ionization (ESI) mass spectra were obtained on a Varian 1200L mass spectrometer at the Environmental Research Training Laboratory (ERTL) at the University of Kentucky or a Thermo Fisher Q-Exactive mass spectrometer at the University of Kentucky Mass Spectrometry Facility. UV/Vis absorption spectra were obtained on a BMG Labtech FLUOstar Omega microplate reader or a Cary 60 spectrometer. Photoluminescence spectra were measured on a Fluorolog-3 spectrofluorometer. Singlet oxygen was detected with a Horiba DSS-IGA020L NIR indium gallium arsenide solid state detector connected to a Horiba Fluoromax Plus-C fluorometer. DNA damage and photochemical experiments were performed using a 470 nm LED array from Elixia ( $10.2 \text{ J}\cdot\text{cm}^{-2}$ ). Agarose gels were digitally imaged using a BioRad ChemiDoc System. Gels were analyzed using BioRad Image Lab. Cytotoxicity assays used a Loctite® Indigo light ( $29.1 \text{ J}\cdot\text{cm}^{-2}$ , ~450 nm) LED array. The Prism software package was used to analyze and plot data.

Synthesis was performed under air unless otherwise stated. Compound **6** and **7** were synthesized as described previously.<sup>1</sup>

## 2. HPLC analysis for purity and photoejection studies

Compounds **1–5** and photoejection products were analyzed using an Agilent 1100 Series HPLC equipped with a model G1311A quaternary pump, G1315B UV diode array detector, and Chemstation software version B.01.03. Chromatographic conditions were optimized on a Phenomenex Luna 5  $\mu\text{m}$  C18(2) 100 Å column fitted with a Phenomenex C18 guard column. Mobile phases of 0.1% formic acid in  $\text{dH}_2\text{O}$  and 0.1% formic acid in HPLC grade  $\text{CH}_3\text{CN}$  were used. Samples of each Ru(II) complex were prepared at a final concentration of 10–100  $\mu\text{M}$  in  $\text{dH}_2\text{O}$  and protected from light (for dark controls and purity analysis) or irradiated to determine the identity of photoejection products.

**Table S1:** HPLC gradient used for compound purity and adduct formation

Time (min)	% $\text{dH}_2\text{O}$ (0.1% formic acid)	% $\text{CH}_3\text{CN}$ (0.1% formic acid)
0	98	2
2	95	5
5	95	5
10	90	10
20	90	10
25	70	30
30	40	60
35	5	95
40	98	2
45	98	2

### 3. Synthesis and characterization of Ru(II) complexes

**Compound 1: [Ru(bpy)<sub>2</sub>(avobenzonate)]PF<sub>6</sub>** [Ru(bpy)<sub>2</sub>Cl<sub>2</sub>]•2H<sub>2</sub>O (150 mg, 0.29 mmol), avobenzene (91 mg, 0.29 mmol) and NEt<sub>3</sub> (44 mg, 0.44 mmol) were added to 10 mL of degassed EtOH : H<sub>2</sub>O (1:1) in a pressure tube. The mixture was stirred at 100 °C for 2 hours, cooled to the room temperature, and transferred into 50 ml of H<sub>2</sub>O. Following this, 1–2 mL of a saturated aqueous KPF<sub>6</sub> solution was added to obtain a red precipitate. The solvent was removed by filtration, washed with water, and with diethyl ether. Yield: 207 mg (81%). <sup>1</sup>H NMR (CD<sub>3</sub>CN): δ 8.74 (t, *J* = 5.6 Hz, 2H), 8.46 (dd, *J* = 8.1, 3.2 Hz, 2H), 8.38 (dd, *J* = 8.1, 3.6 Hz, 2H), 8.03 (t, *J* = 8.0 Hz, 2H), 7.90 (t, *J* = 6.8 Hz, 2H), 7.79–7.85 (m, 2H), 7.64 (d, *J* = 8.8 Hz, 2H), 7.52–7.60 (m, 4H), 7.33 (d, *J* = 8.4 Hz, 2H), 7.15–7.20 (m, 2H), 6.82 (d, *J* = 8.8 Hz, 2H), 6.68 (s, 1H), 3.77 (s, 3H), 1.26 (s, 9H). <sup>13</sup>C NMR (101 MHz, CD<sub>3</sub>CN): δ 181.37, 181.17, 162.73, 160.13, 160.12, 158.84, 158.82, 154.95, 154.45, 151.15, 138.01, 137.46, 135.91, 135.89, 133.09, 129.24, 127.20, 127.15, 126.26, 126.24, 126.17, 124.09, 123.97, 123.94, 118.31, 114.45, 94.07, 56.11, 35.44, 31.28. Purity by HPLC = 99 %. ESI MS calcd for C<sub>40</sub>H<sub>37</sub>N<sub>4</sub>O<sub>3</sub>Ru [M]<sup>+</sup> 723.19; found 723.3 [M]<sup>+</sup>. UV/Vis (CH<sub>3</sub>CN): λ<sub>max</sub> (ε × 10<sup>3</sup>) 500 nm (13.2).

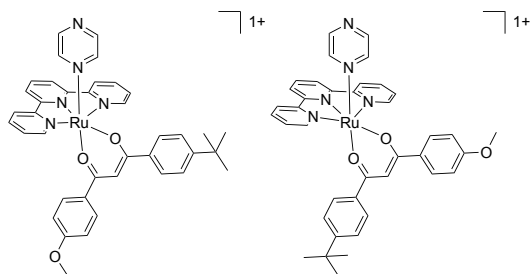
**Compound 2: [Ru(dip)<sub>2</sub>(avobenzonate)]PF<sub>6</sub>** [Ru(dip)<sub>2</sub>Cl<sub>2</sub>] (100 mg, 0.12 mmol), avobenzene (37 mg, 0.12 mmol) and NEt<sub>3</sub> (18 mg, 0.18 mmol) were added to 15 mL of degassed EtOH : H<sub>2</sub>O (2:1) in a pressure tube. The mixture was stirred at 100 °C for 2 hours, cooled to the room temperature, and transferred into 50 ml of H<sub>2</sub>O. Following this, 1–2 mL of a saturated aqueous KPF<sub>6</sub> solution was added to obtain a purple precipitate. The solvent was removed by filtration. The purification of the solid was carried out by flash chromatography eluting with MeCN (Alumina N, loaded in MeCN). The product fractions were collected and the solvent was removed under reduced pressure to give the product as a solid. Yield: 95 mg (65%). <sup>1</sup>H NMR (CD<sub>3</sub>CN): δ 9.26 (dd, *J* = 5.4, 3.8 Hz, 2H), 8.22 (dd, *J* = 9.8, 5.6 Hz, 2H), 8.05–8.14 (m, 4H), 7.86 (dd, *J* = 5.4, 1.6 Hz, 2H), 7.51–7.72 (m, 24H), 7.38 (dd, *J* = 6.8, 5.6 Hz, 2H), 7.29 (d, *J* = 8.6 Hz, 2H), 6.82 (s, 1H), 6.77 (d, *J* = 8.8 Hz, 2H), 3.72 (s, 3H), 1.21 (s, 9H). <sup>13</sup>C NMR (125 MHz, CD<sub>3</sub>CN): δ 181.68, 181.43, 162.77, 155.02, 154.70, 151.96, 151.39, 150.53, 150.49, 148.75, 147.15, 147.11, 138.10, 137.24, 137.01, 133.12, 130.93, 130.80, 130.39, 130.28, 130.06, 129.98, 129.45, 129.23, 129.21, 129.20, 129.17, 127.41, 126.63, 126.60, 126.56, 126.53, 126.17, 125.56, 125.53, 114.44, 94.29, 56.11, 35.42, 31.26. Purity by HPLC = 98 %. ESI MS calcd for C<sub>68</sub>H<sub>53</sub>N<sub>4</sub>O<sub>3</sub>Ru [M]<sup>+</sup> 1075.32; found 1075.32 [M]<sup>+</sup>. UV/Vis (CH<sub>3</sub>CN): λ<sub>max</sub> (ε × 10<sup>3</sup>) 510 nm (21.3).

**Compound 3: Li<sub>3</sub>[Ru(bps)<sub>2</sub>(avobenzonate)]<sup>3-</sup>** Li<sub>4</sub>[Ru(bps)<sub>2</sub>Cl<sub>2</sub>] (120 mg, 0.08 mmol), avobenzene (31 mg, 0.1 mmol) and NEt<sub>3</sub> (51 mg, 0.5 mmol) were added to 7 mL of degassed EtOH : H<sub>2</sub>O (2:5) in a pressure tube. The mixture was stirred at 100 °C for 2 hours, cooled to the room temperature, and transferred into 300 mL of acetone to obtain a precipitate. The solvent was removed by filtration. The purification of the solid was carried out by flash chromatography (silica, loaded in MeCN). A gradient was run, and the pure complex eluted at 10% H<sub>2</sub>O in MeCN. The product fractions were concentrated under reduced pressure, and transferred into 100 ml of acetone. The solvent was removed under reduced pressure to give the product as a solid. Yield: 32 mg (22%). <sup>1</sup>H NMR (CD<sub>3</sub>OD): δ 9.34 (s, 2H), 8.33–7.29 (m, 33H), 6.86 (s, 1H), 6.78 (s, 2H), 3.72 (s, 2H), 1.22 (s, 9H). UV/Vis (CH<sub>3</sub>CN): λ<sub>max</sub> (ε × 10<sup>3</sup>) 500 nm (14.1). ESI MS calcd for C<sub>68</sub>H<sub>49</sub>N<sub>4</sub>O<sub>15</sub>RuS<sub>4</sub> [M]<sup>3-</sup> 463.7; found 463.7.

Sulfonated ligands are known to cause challenges in characterization. Several metal complexes with sulfonated ligands have been characterized only by <sup>1</sup>H NMR and MS<sup>2-4</sup>, and in some cases it was only possible to get MS data.<sup>5</sup>



#### Compound 4: [Ru(tpy)(avobenzonate)(pyrazine)]PF<sub>6</sub>



[[Ru(tpy)(avobenzonate)Cl] (50 mg, 0.074 mmol) and 15-fold excess of pyrazine (88 mg, 1.1 mmol) were added to 10 mL of degassed EtOH in a pressure tube. The mixture was stirred at 80 °C for 3 hours, cooled to the room temperature, and transferred into 50 mL of H<sub>2</sub>O. Following this, 1–2 mL of a saturated aqueous KPF<sub>6</sub> solution was added to obtain a red precipitate that was isolated by filtration to yield a mixture of isomers which were not separated. Yield: 56 mg (88%). <sup>1</sup>H NMR (acetone-d<sub>6</sub>): δ 8.65–8.73 (m, 6H), 8.51 (d, *J* = 3.7 Hz, 2H), 8.43 (d, *J* = 8.8 Hz, 1.2H), 8.37 (d, *J* = 8.4 Hz, 0.8H), 8.28 (d, *J* = 3.6 Hz, 2H), 8.10–8.16 (m, 3H), 7.66–7.73 (m, 3H), 7.43 (d, *J* = 8.8 Hz, 0.8H), 7.36 (d, *J* = 8.4 Hz, 1.2H), 7.15–7.20 (m, 2H), 6.90 (s, 0.4H), 6.89 (s, 0.6H), 6.69 (d, *J* = 8.8 Hz, 1H), 3.97 (s, 1.8H), 3.71 (s, 1.2H), 1.44 (s, 3.4H), 1.18 (s, 5.4H). <sup>13</sup>C NMR (125 MHz, acetone-d<sub>6</sub>): δ 182.46, 182.19, 182.02, 163.19, 162.71, 161.58, 160.16, 155.02, 154.60, 151.82, 151.78, 149.41, 145.99, 138.76, 138.24, 137.21, 133.39, 133.30, 132.21, 130.09, 129.07, 128.77, 128.04, 127.05, 126.41, 125.78, 124.54, 123.44, 114.75, 114.12, 93.50, 93.41, 55.98, 55.67, 35.55, 35.23, 31.52, 31.23. Purity by HPLC = 98 %. ESI MS calcd for C<sub>39</sub>H<sub>36</sub>N<sub>5</sub>O<sub>3</sub>Ru [M]<sup>+</sup> 724.19; found 723.3 [M]<sup>+</sup>. UV/Vis (CH<sub>3</sub>CN): λ<sub>max</sub> (ε × 10<sup>3</sup>) 435 nm (7.8).

#### Compound 5: [Ru(tpy)(avobenzonate)Cl]

A mixture of [Ru(tpy)Cl<sub>3</sub>] (220 mg, 0.5 mmol), avobenzonate (155 mg, 0.5 mmol), NEt<sub>3</sub> (760 mg, 7.5 mmol) were added to 30 mL of degassed EtOH : H<sub>2</sub>O (1:1) in a pressure tube. The mixture was stirred at 90 °C for 5 hours, cooled to the room temperature, transferred into 100 mL of DCM, and washed with 100 mL of H<sub>2</sub>O. The organic fraction was isolated, and the solvent removed under reduced pressure. The purification of the solid was carried out by flash chromatography (alumina N, loaded in DCM). A gradient was run, and the pure complex eluted at 5% MeOH in DCM. The product fractions were collected and the solvent was removed under reduced pressure to give the product as a mixture of isomers which were not separated. Yield: 97 mg (29%). <sup>1</sup>H NMR (acetone-d<sub>6</sub>): δ 8.84 (t, *J* = 5.5 Hz, 2H), 8.40–8.48 (m, 6H), 7.91 (t, *J* = 7.6 Hz, 2H), 7.54–7.66 (m, 4H), 7.08–7.25 (m, 4H), 6.74 (s, 0.4H), 6.73 (s, 0.6H), 6.59–6.62 (m, 1H), 3.96 (s, 1.8H), 3.66 (s, 1.2H), 1.45 (s, 3.6H), 1.15 (s, 5.4H). <sup>13</sup>C NMR (101 MHz, CDCl<sub>3</sub>): δ 161.56, 160.76, 158.94, 153.60, 153.50, 153.04, 152.83, 140.70, 138.32, 137.36, 135.87, 135.67, 133.52, 132.67, 128.98, 127.53, 126.86, 125.77, 125.63, 125.24, 125.06, 120.83, 120.73, 114.00, 113.62, 55.64, 55.42, 35.22, 34.91, 31.34, 31.11. ESI MS calcd for C<sub>35</sub>H<sub>32</sub>ClN<sub>3</sub>O<sub>3</sub>Ru [M]<sup>+</sup> 679.12; found 679.3 [M]<sup>+</sup>. UV/Vis (CH<sub>3</sub>CN): λ<sub>max</sub> (ε × 10<sup>3</sup>) 570 nm (7.8).

#### 4. Counterion exchange

Prior to biological testing and all experiments performed in aqueous media, metal complexes possessing counterions were converted to salts containing the chloride counterion by dissolving ~20 mg of product in 1–

2 mL methanol. The dissolved product was loaded onto an Amberlite IRA-410 chloride ion exchange column, eluted with methanol, and the solvent was removed under reduced pressure.

## 5. Photoejection studies

The quantum yield for the complex **4**, with chloride counterions, was determined by an HPLC approach as has been described previously.<sup>6</sup> The use of HPLC allows for quantitation of the species by integration of the peak areas in the chromatograms obtained at various time points. The Ru(II) complex was irradiated in a 96-well plate with a 470 nm LED at a concentration of 100  $\mu$ M with a path length of 0.5 cm. The photon flux of the lamp in the plate was determined by ferrioxalate actinometry ( $1.77 \cdot 10^{-8}$  E/s).

The absorbance of complex at a concentration of 100  $\mu$ M at 470 nm was 0.61, providing a photon absorption probability  $F = 0.75$ . Therefore, the moles of photon absorbed have been calculated as the product of photons irradiated and photon absorption probability.

The kinetics for ligand ejection from **4** (30  $\mu$ M) was determined in triplicate in a Greiner UV clear half-area 96-well plate in water, 1X PBS, and opti-MEM. The plate was positioned 12 inches below a 470 nm LED array and spectra were collected after set time points for a total of 4 hours. The normalized change in absorbance was plotted versus time to give the  $t_{1/2}$  of ligand loss.

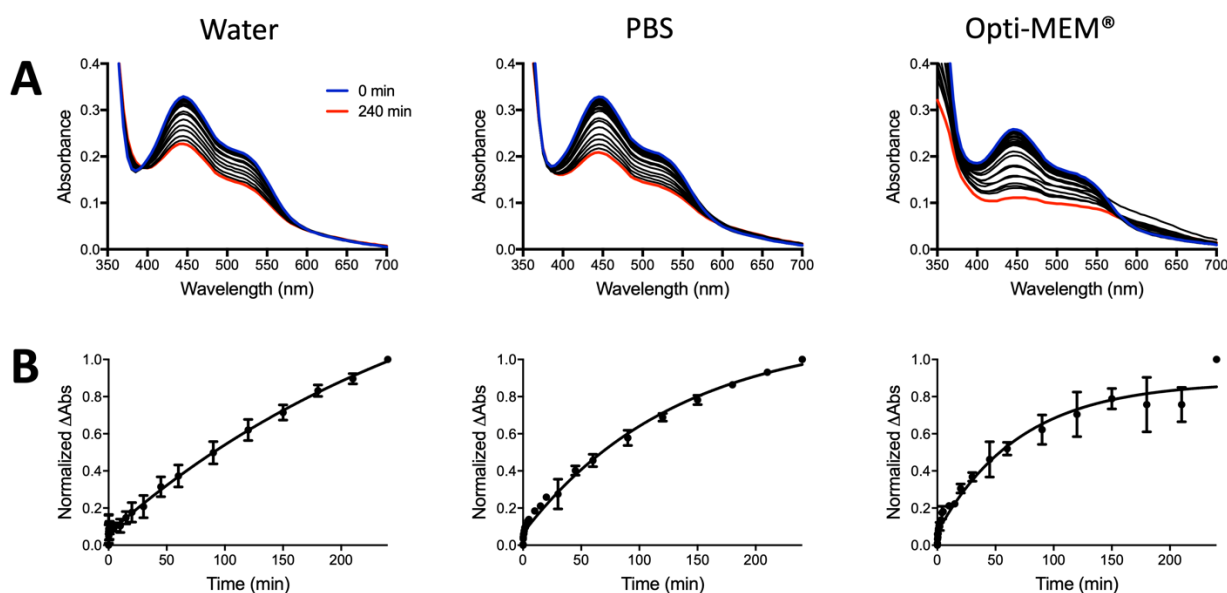


**Figure S1.** Photoejection kinetics in water, 1X PBS, and Opti-MEM for compound **4**. (A) UV/Vis absorbance changes during irradiation with 470 nm ( $37 \text{ J} \cdot \text{cm}^{-2}$ ) 0 min (blue line) to 240 min (red line). (B) Monoexponential plots of the change in absorbance over time.

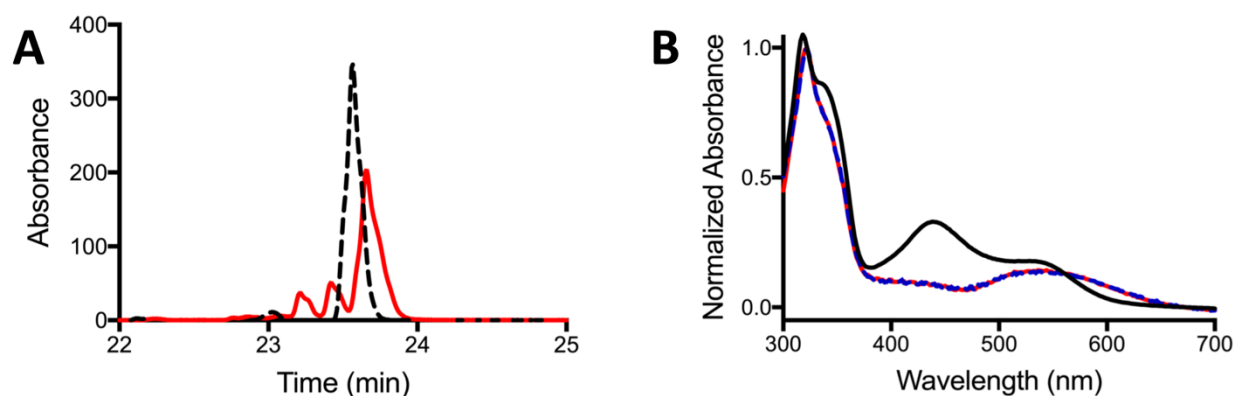


**Figure S2** (A) HPLC trace of **4** prior to irradiation (black dash line) and after 4 h of irradiation with 470 nm ( $147 \text{ J/cm}^2$ ) light (red line). (B) UV/Vis absorbance analysis of photochemical products: **4** before light activation (black line), the photochemical product eluted at 23.2 min (blue dash), and the photochemical product eluted at 23.4 min (red line). Note the retention time of the major peaks in (A) are shifted due to slight variation ( $< 0.4\%$  difference) in the HPLC retention times between different acquisitions of the same compound. The identity of these peaks has been confirmed via absorbance profile of each peak.

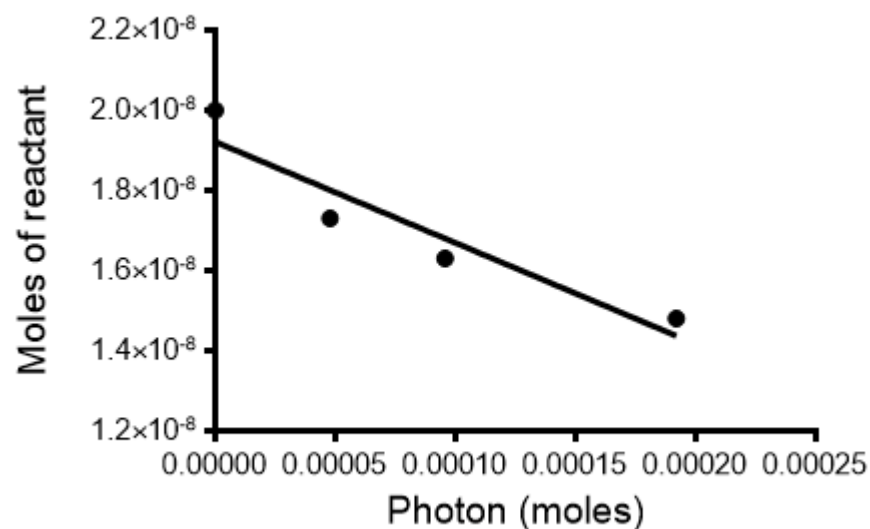


**Figure S3.** Linear regression for moles of reactant vs. moles of photons absorbed for complex **5** based on HPLC.

**Table S2:** Parameters used in determining the quantum yield of **4** by HPLC.

Time (s)	Photons irradiated	Photons absorbed	Compound <b>4</b>	
			Area	Moles in well
0	0	0	2522.8	2.00E-08
3600	6.37E-05	4.79E-05	2178.3	1.73E-08
7200	1.27E-04	9.58E-05	2051.5	1.63E-08
14400	2.55E-04	1.92E-04	1869.1	1.48E-08

## 6. Cell Culture.

HL60 human leukemic cells were obtained from ATCC, maintained in Iscove's media, and supplemented with 10% FBS and 1X penicillin–streptomycin (pen-strep). DU145 and MIA PaCa-2 cell lines were obtained from ATCC, maintained in DMEM media, and supplemented with 10% FBS containing 1X penicillin–streptomycin and maintained at 37 °C with 5% CO<sub>2</sub>. Cells were incubated at 37 °C and 5% CO<sub>2</sub>. An extracellular solution was used for cell cytotoxicity studies in place of opti-MEM™ to prevent cellular damage from light irradiation. The extracellular solution was made with 10 mM HEPES, 10 mM glucose, 1.2 mM CoCl<sub>2</sub>, 1.2 mM MgCl<sub>2</sub>, 3.3 mM KH<sub>2</sub>PO<sub>4</sub>, 0.83 mM K<sub>2</sub>HPO<sub>4</sub>, and 145 mM NaCl in water.

## 7. Cytotoxicity Assay

HL60 cells were plated at 30,000 cell per well in Opti-MEM media with 1% FBS and pen-strep in 96-well plates. DU145 and MIA PaCa-2 cells were plated at 2,000 cell per well in DMEM media with 10% FBS and pen-strep in 96-well plates and incubated overnight. Media was aspirated and replaced with extracellular solution. Compounds were serially diluted in opti-MEM with 1% FBS and pen-strep in a 96-well plate and then added to the cells. They were then irradiated with 29.1 J/cm<sup>2</sup> light (>450 nm using the Indigo LED) for 1 minute or kept in the dark. The cells were incubated with the compounds for 72 h followed by the addition of resazurin. The plates were incubated for 3 h and then read on a SpectraFluor Plus plate reader with an excitation filter of 535 nm and emission of 595 nm.

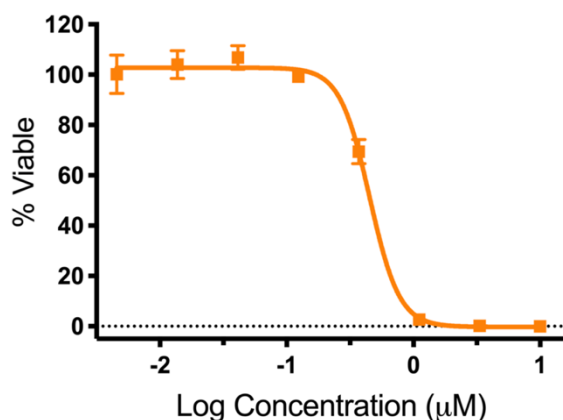


**Figure S4.**Light-activated cytotoxicity dose response of **5**. Irradiated with Indigo light (>450 nm 29.1 J/cm<sup>2</sup> light) for 60 s.

### **8. Aqueous stability.**

Measured by UV/Vis: The aqueous stability of complexes **8–10** was studied at 37 °C as 30 µM solutions in DI-water, Opti-MEM™ with 2% fetal bovine serum, and 1X PBS buffer. Each solution was measured in triplicate in a 96-well plate and monitored by UV/vis absorbance over the course of 72 hours. Solvent evaporation was slowed during incubation by covering plate with a Breath-Easy® membranes, which were removed before UV/Vis absorbance measurements.

Measured by HPLC: Compounds **1, 2, 4, and 7** were diluted in water to 100 µM. Their HPLC chromatograms were recorded and the samples were incubated at 37 °C for 72 h. Chromatograms were recorded for each compound. The solution of each sample was removed and the remaining small amount of precipitate on the walls of the vial was dissolved in 60 µL of 1:1 MeCN: DMSO (V:V) and a chromatogram obtained.

### **9. DNA gel electrophoresis.**

Ru(II) complexes were serially diluted 1:2 to give final concentrations of 0, 7.8, 15.6, 31.3, 62.5, 125, 250, and 500 µM of compound with 40 µg/mL of pUC19 plasmid in 10 mM phosphate buffer pH 7.4 in a 96-well plate or PCR tubes. The dark control samples were removed prior to exposure of the plasmid solution to light. The samples were then irradiated with 470 nm light for 1 h ( $37 \text{ J} \cdot \text{cm}^{-2}$ ). Irradiated and control samples were incubated overnight at 37 °C. 6X DNA loading dye was added to each sample and the plasmid samples were resolved on a 1% agarose gel in 1X Tris-Acetate (TA) buffer, with 0.3 µg of plasmid loaded per lane. The samples were run for 75 min at 100 mV followed by staining the gel with a solution of ethidium bromide in 1X TA buffer for 40 min. The gels were then destained in 1X TA buffer for 30 min and digitally imaged.

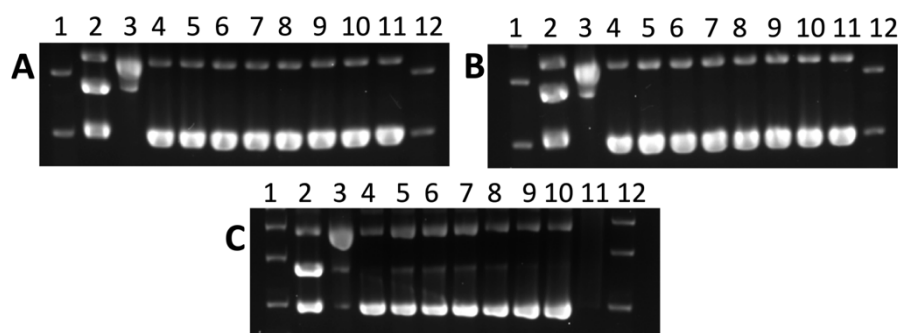


**Figure S5.** Agarose gel electrophoresis of pUC19 plasmid ( $40 \mu\text{g mL}^{-1}$ ; 10 mM phosphate buffer, pH 7.4) with (A) compound **3** without light activation, (B) with light activation (470 nm,  $37 \text{ J}\cdot\text{cm}^{-2}$ ), (C) compound **7** without light activation. Lanes 1 and 12, DNA molecular weight standard; lane 2, linear pUC19; lane 3, relaxed circle  $[\text{Cu}(\text{phen})_2]$  reaction with pUC19; lanes 4–11, 0, 7.8, 15.6, 31.25, 62.5, 125, 250, and  $500 \mu\text{M}$  compound.

#### 10. Calf Thymus DNA interactions.

Complexes were diluted to  $20 \mu\text{M}$  in phosphate buffer (50 mM, pH = 7.4) and titrated with calf thymus DNA (ctDNA) until saturation was reached as indicated by the absorbance profile remaining stable. The solution was incubated at room temperature for 5 min after every addition before UV/Vis spectra were recorded. The change of absorbance was plotted as previously described.<sup>7</sup>

#### 11. Singlet Oxygen detection.

The singlet oxygen generation of the Ru(II) complexes was measured by monitoring the phosphorescence of  $^1\text{O}_2$  at 1275 nm in  $\text{CD}_3\text{OD}$ . An excitation source of 450 nm was used for all compounds. Isoabsorptive solutions were tested, with absorbance of  $\sim 0.2$  at 450 nm. Excitation and emission slits spectral widths were set to 29 nm. Integration was set to 5 seconds and emission was collected from 1220–1350 nm.

#### 12. Toxicity assays in zebrafish

Animal studies were approved under the University of Kentucky's Institutional Animal Care and Use Committee, protocol 2019-3399. Healthy 2 day post fertilization (dpf) Casper strain zebrafish larvae were pipetted into 96-well plates, at 1 larvae per well in  $150 \mu\text{L}$  1X E3 media (5mM NaCl, 0.17mM KCl, 0.33mM  $\text{MgSO}_4$  in dH<sub>2</sub>O). Compounds were prepared at 2X of the desired concentration in E3 media and  $150 \mu\text{L}$  added to each well. Plates were incubated in the dark for a 96hr, with drug refreshed during media change at 48hr. Animals were imaged using a Vertebrate Automated Imaging System (Union Biometrica) as previously described.<sup>8</sup> Care was taken to keep all compounds in the dark throughout their use, and each compound was tested in triplicate at two concentrations.

### 13. Additional Figures

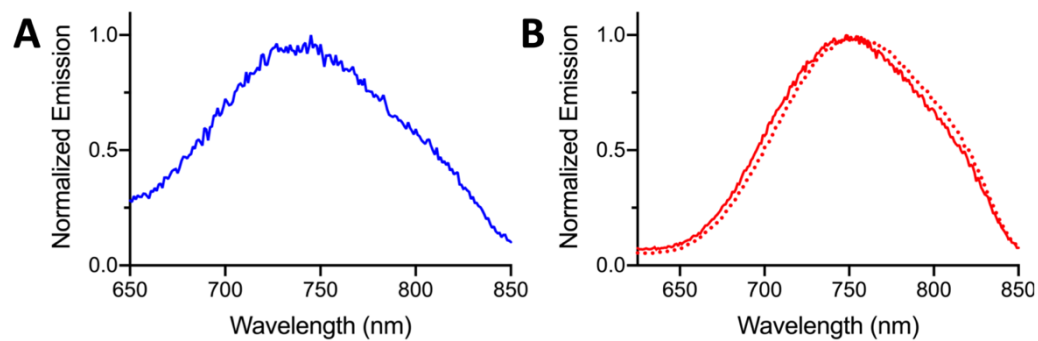


**Figure S6.** Emission spectra in acetonitrile (line) and water (dots) of compounds **1** (A) and **2** (B).

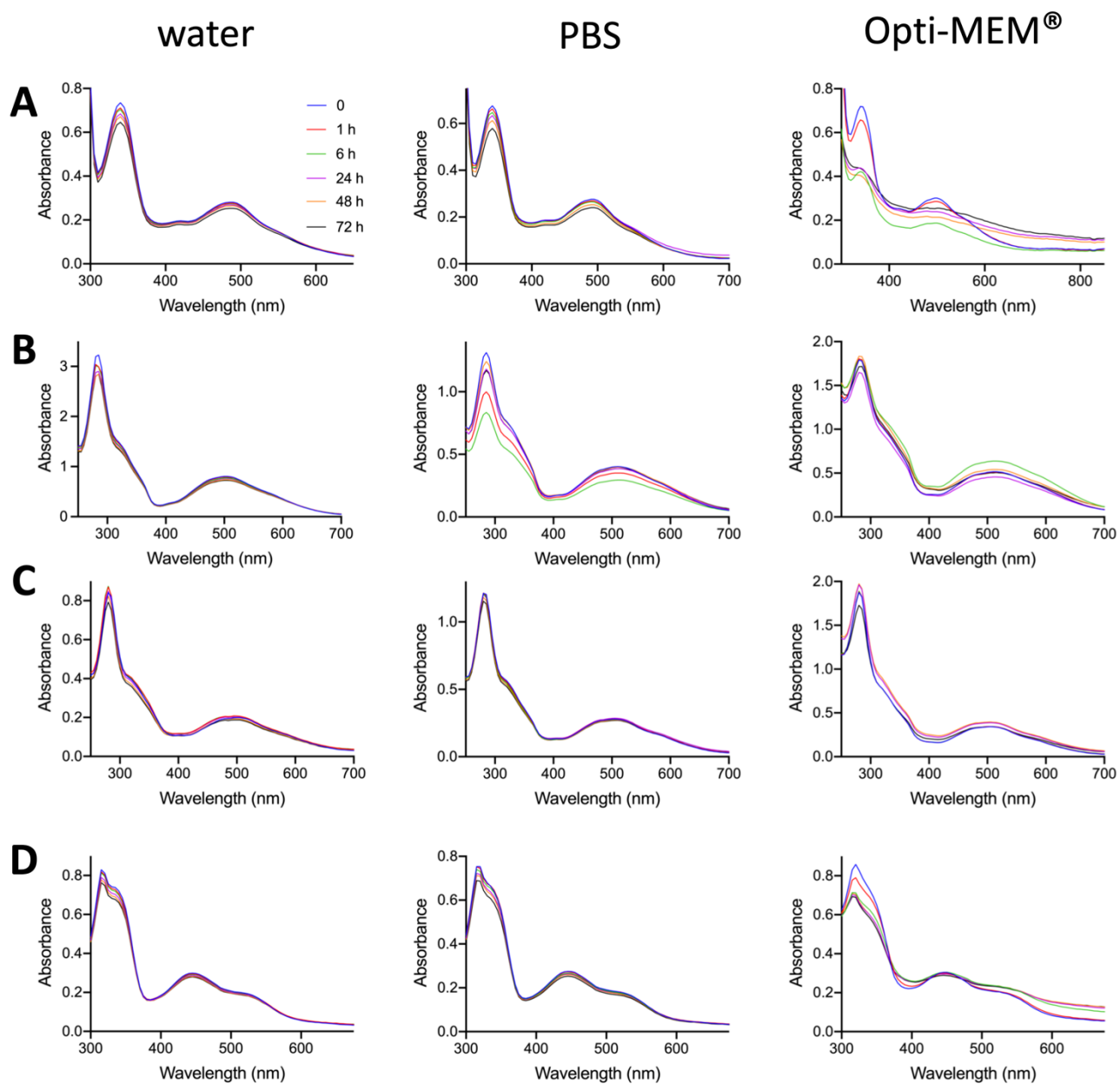


**Figure S7.** Aqueous stability over the course of 72 h at 37 °C monitored by UV/Vis in water, 1X PBS and Opti-MEM for compounds **1** (A), **2** (B), **3** (C), and **4** (D).



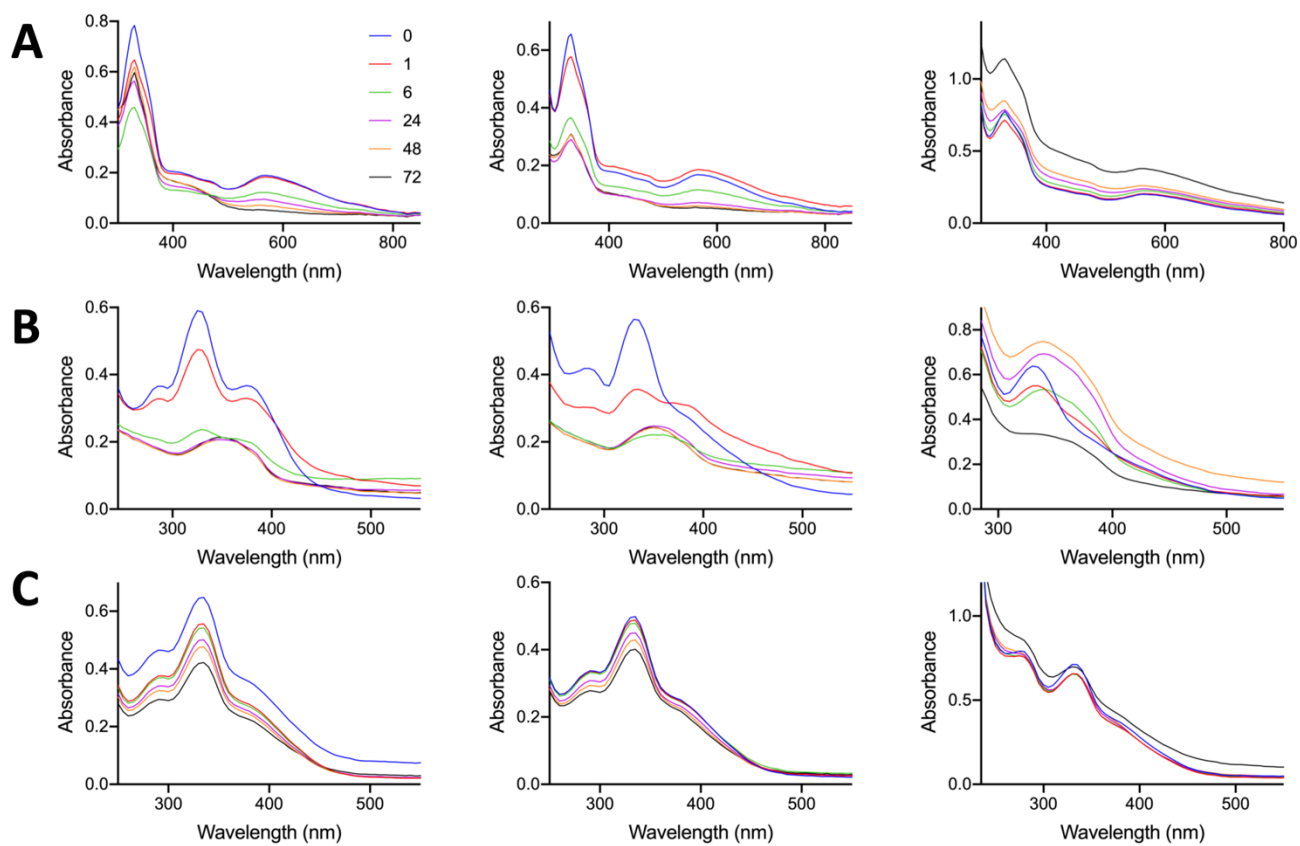


**Figure S8.** Aqueous stability over the course of 72 h at 37 °C monitored by UV/Vis in water, 1X PBS and Opti-MEM for compounds **5** (A), **6** (B), and **7** (C)

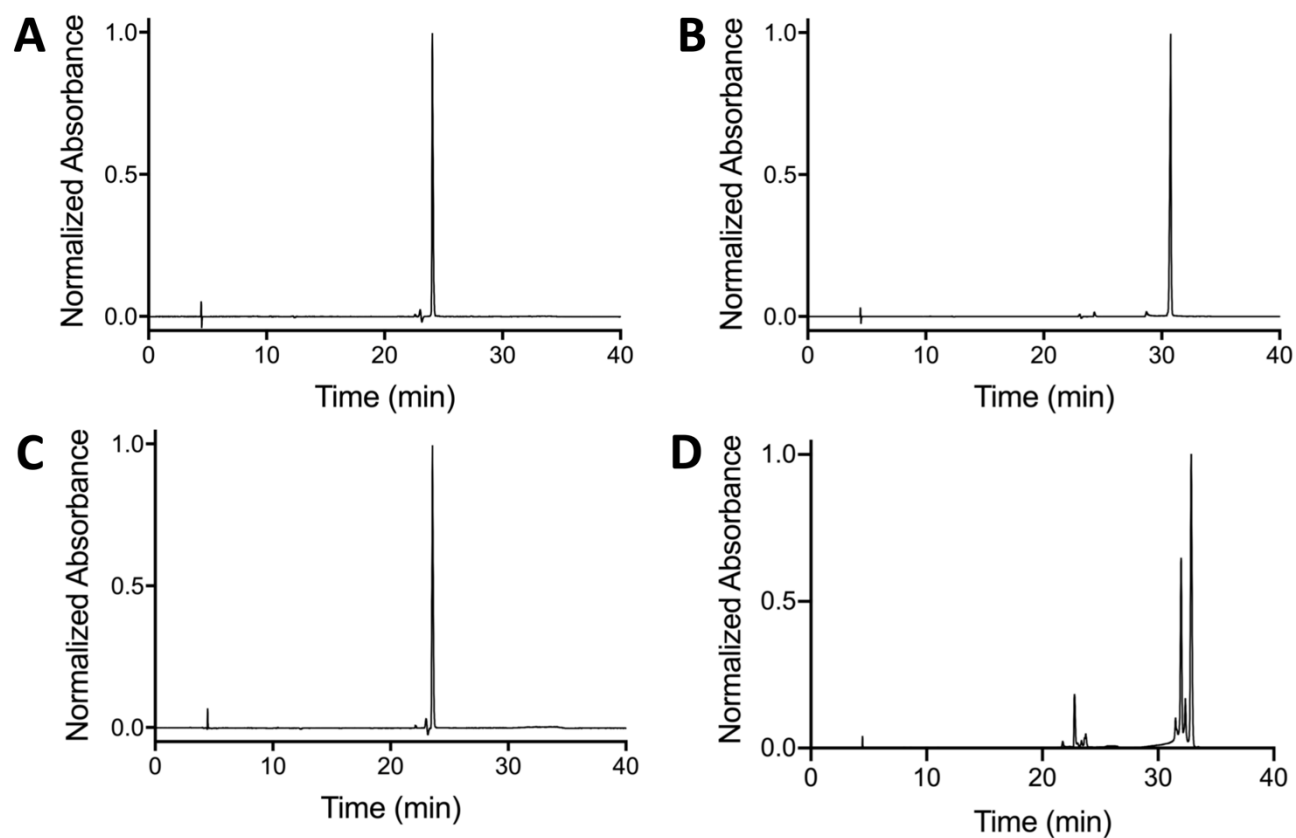


**Figure S9.** HPLC analysis of purity of compounds **1** (A), **2** (B), **4** (C), **5** (D). No HPLC was obtained for compound **3** as it is highly hydrophilic and has only weak interactions with the C18 column. As was seen in the aqueous stability experiments, compound **5** decomposes in the presence of water during elution.

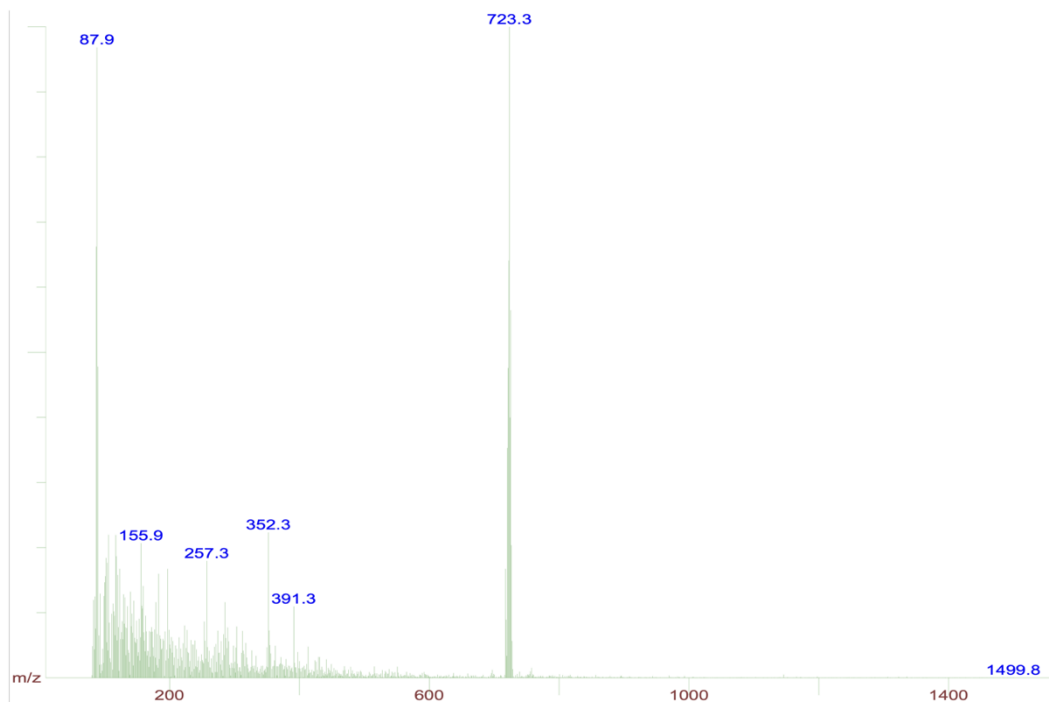


**Figure S10.** ESI-MS of compound **1**. Calcd value for  $\text{C}_{40}\text{H}_{37}\text{N}_4\text{O}_3\text{Ru} [\text{M}]^+$  723.19; found 723.3.

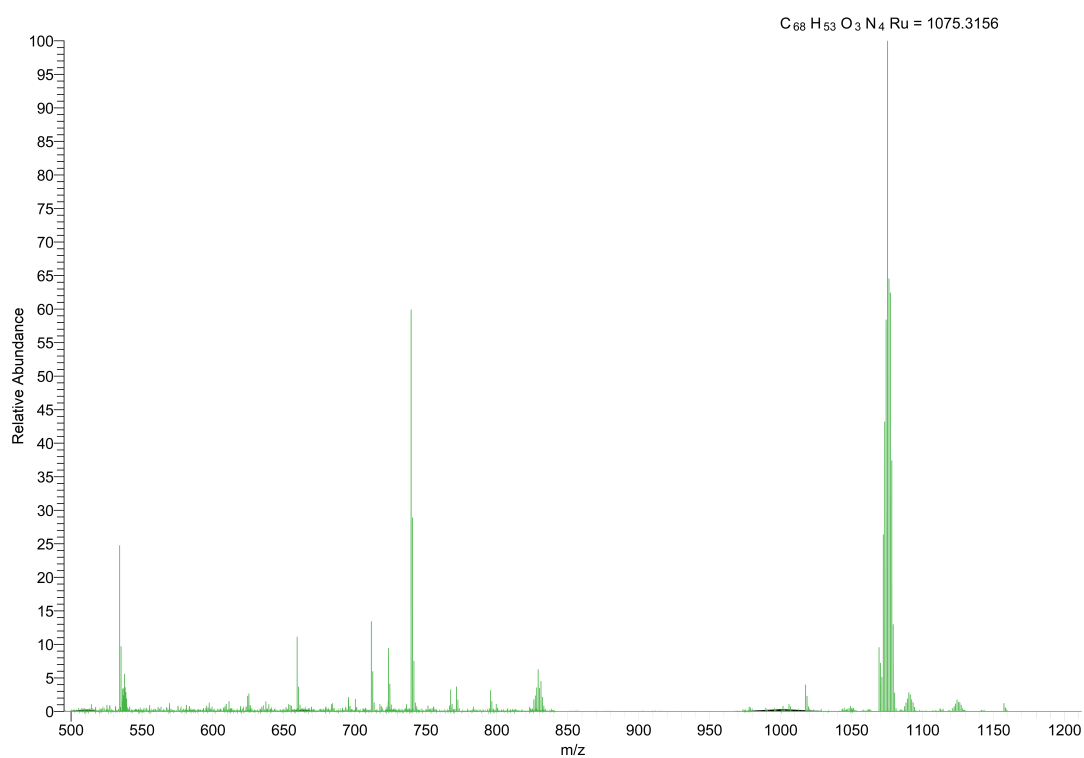


**Figure S11.** ESI-MS of compound **2**. Calcd value for  $\text{C}_{68}\text{H}_{53}\text{N}_4\text{O}_3\text{Ru} [\text{M}]^+$  1075.32; found 1075.32.

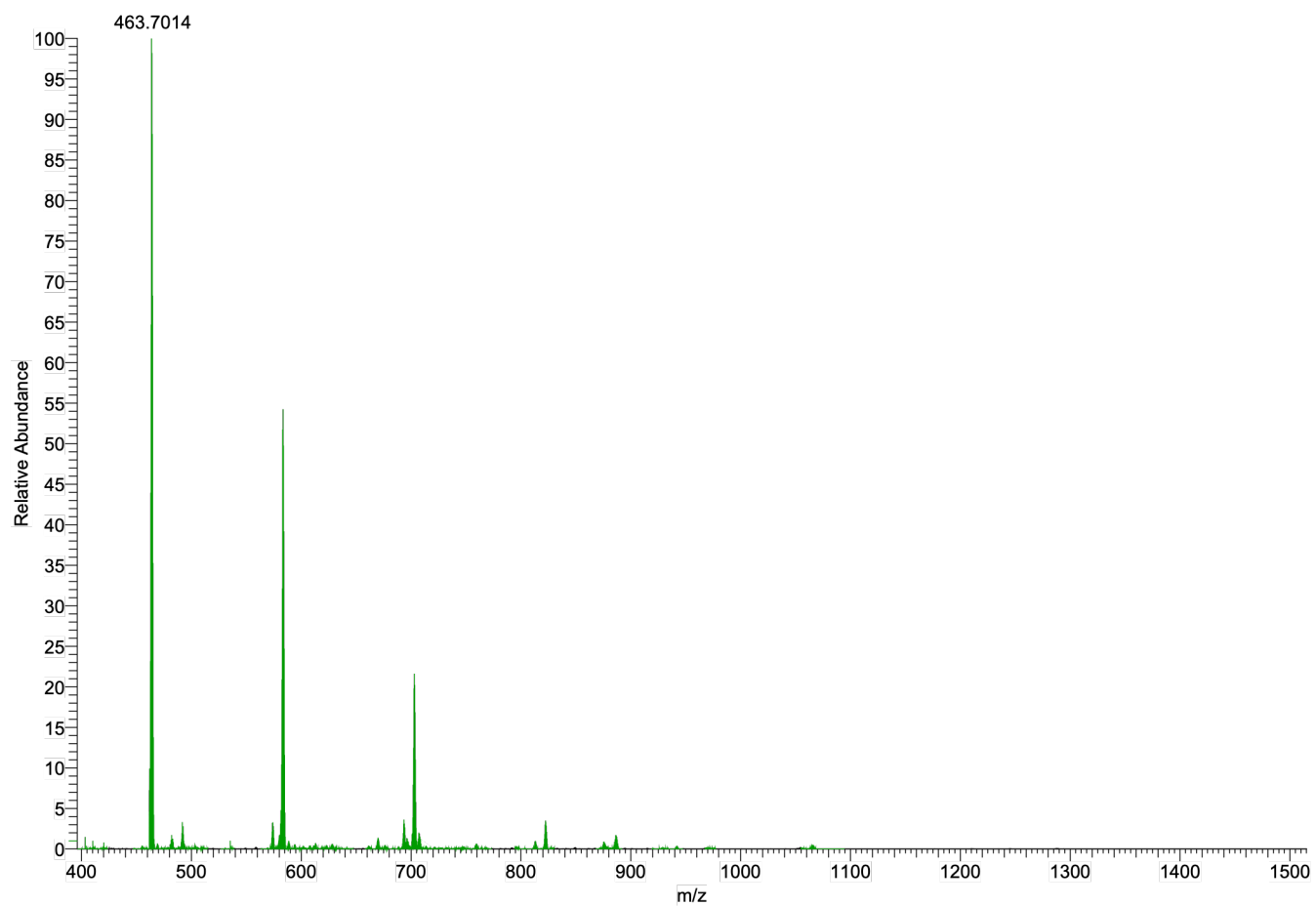


**Figure S12.** ESI-MS of compound **3**. Calcd for  $\text{C}_{68}\text{H}_{49}\text{N}_4\text{O}_{15}\text{RuS}_4$   $[\text{M}]^{3-}$  463.7; found 463.7.

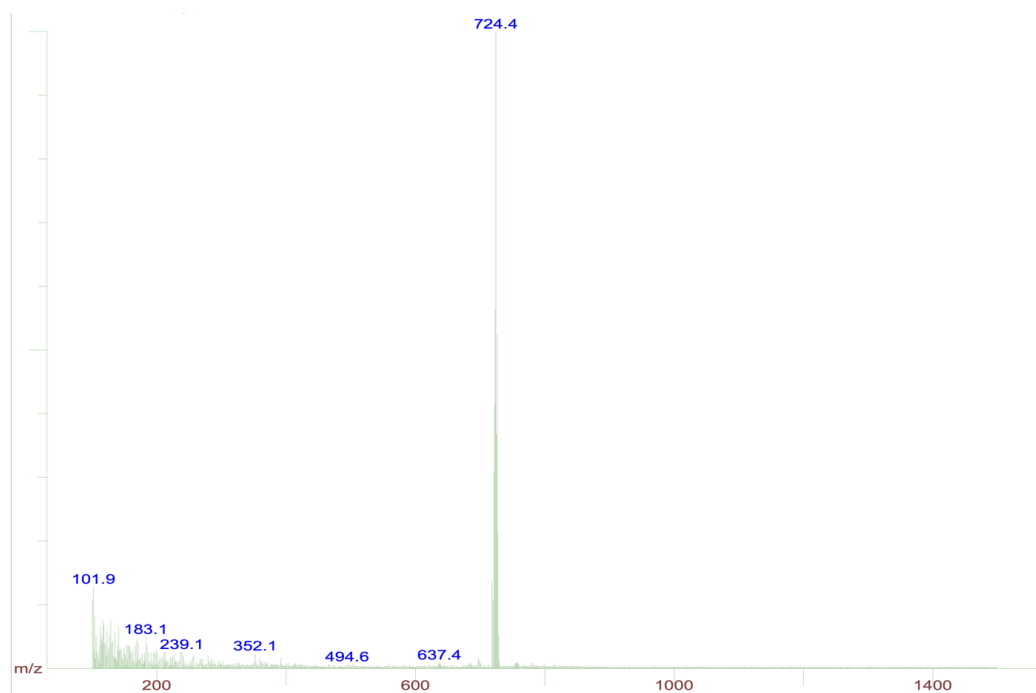


**Figure S13.** ESI-MS of compound **4**. Calcd for  $\text{C}_{39}\text{H}_{36}\text{N}_5\text{O}_3\text{Ru}$   $[\text{M}]^+$  724.19; found 724.4  $[\text{M}]^+$ .

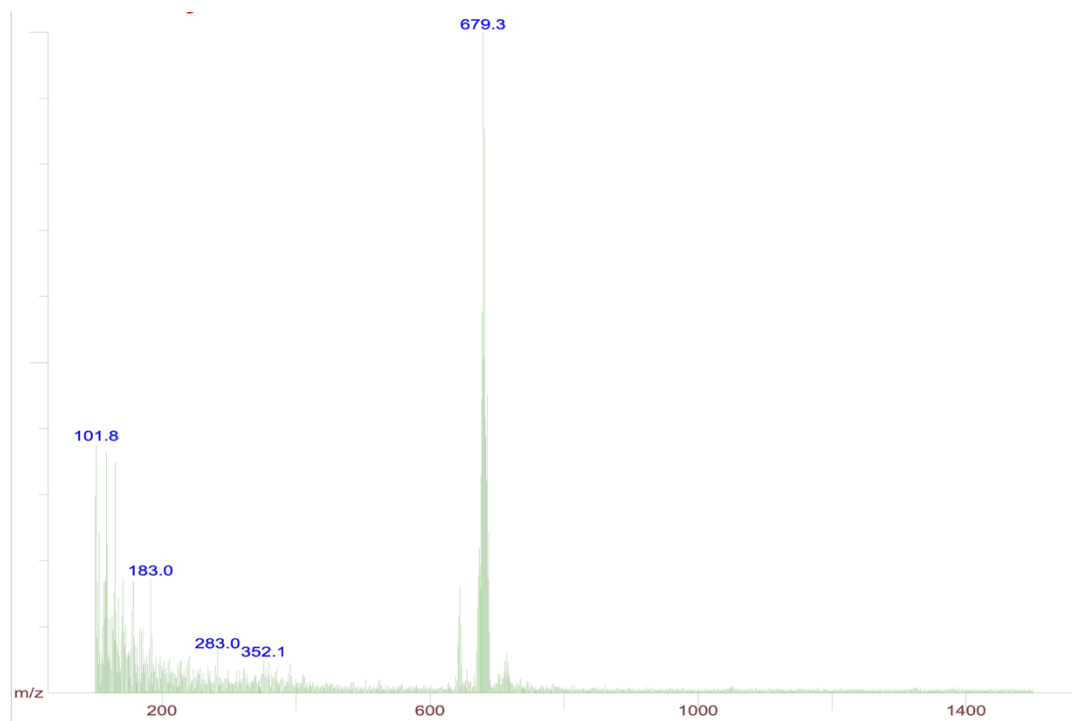


**Figure S14.** ESI-MS of compound **5**. Calcd for  $\text{C}_{35}\text{H}_{32}\text{ClN}_3\text{O}_3\text{Ru}$   $[\text{M}]^+$  679.12; found 679.3  $[\text{M}]^+$ .

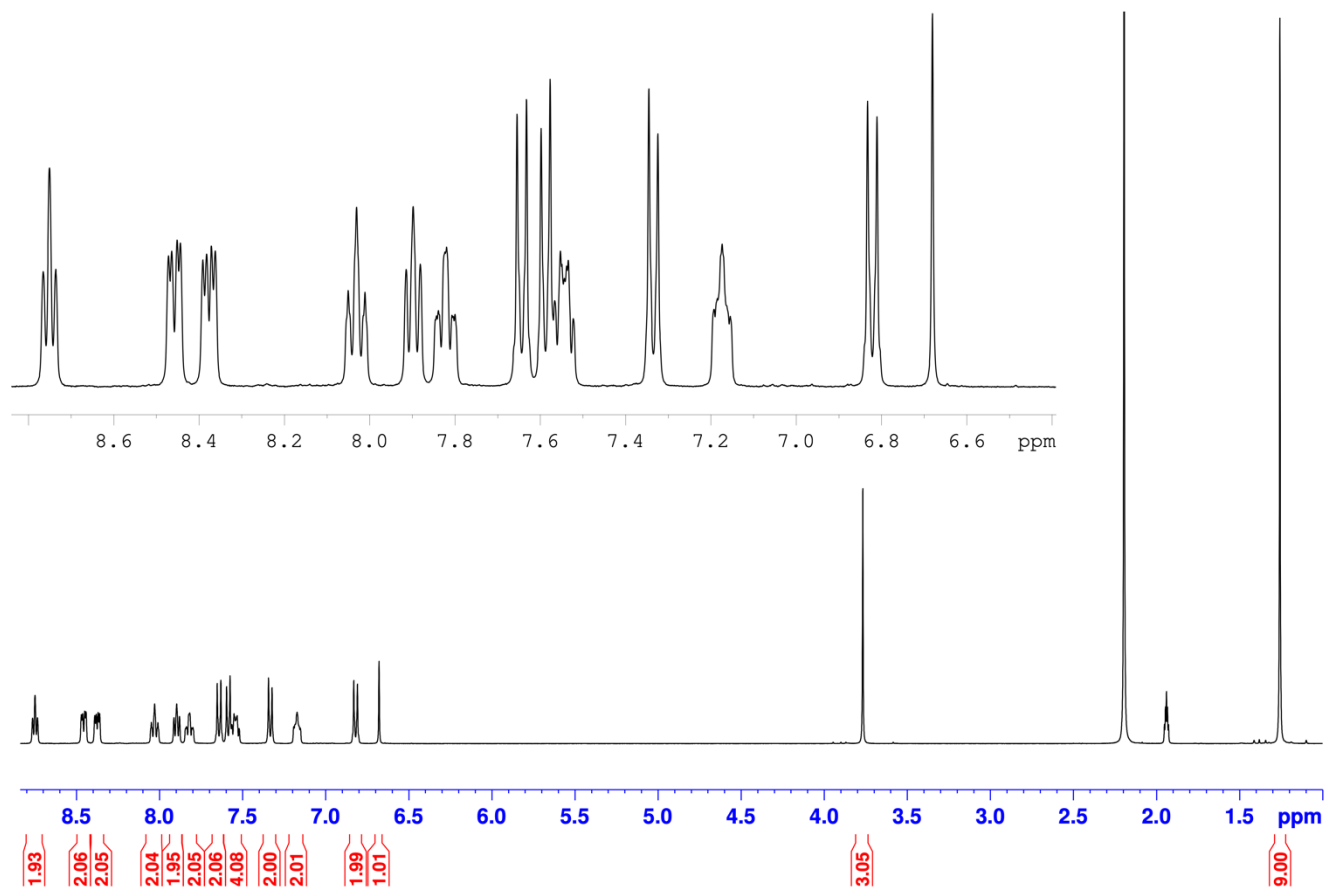


**Figure S15.**  $^1\text{H}$  NMR of compound **1** in  $\text{CD}_3\text{CN}$ .

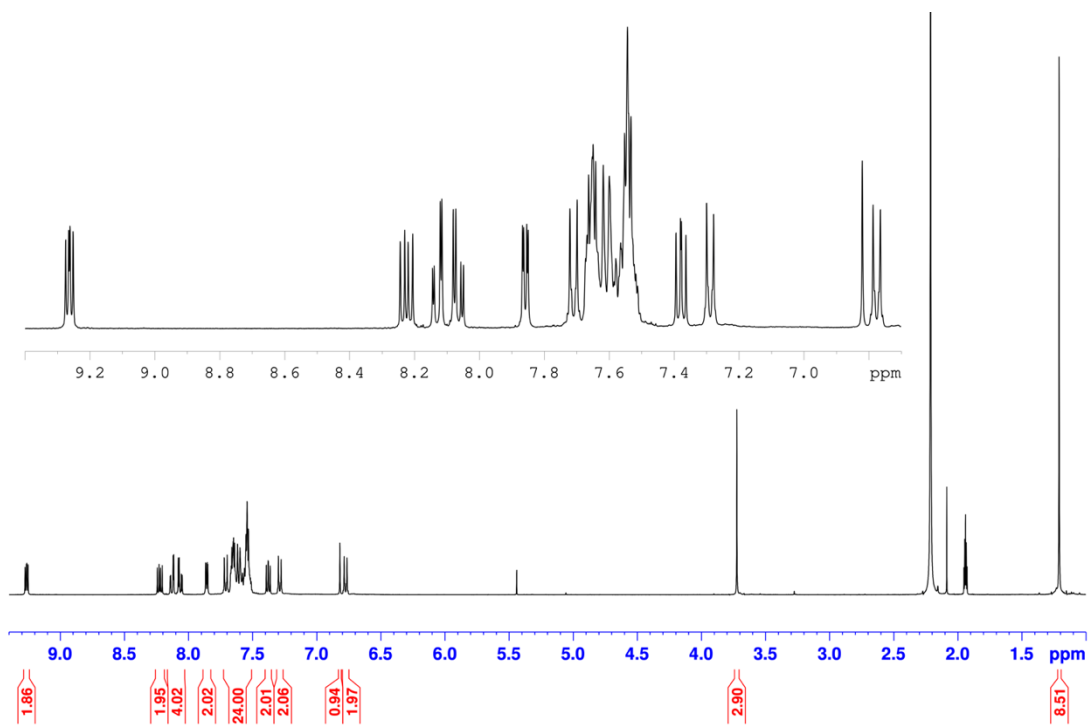


**Figure S16.** <sup>1</sup>H NMR of compound **2** in CD<sub>3</sub>CN.

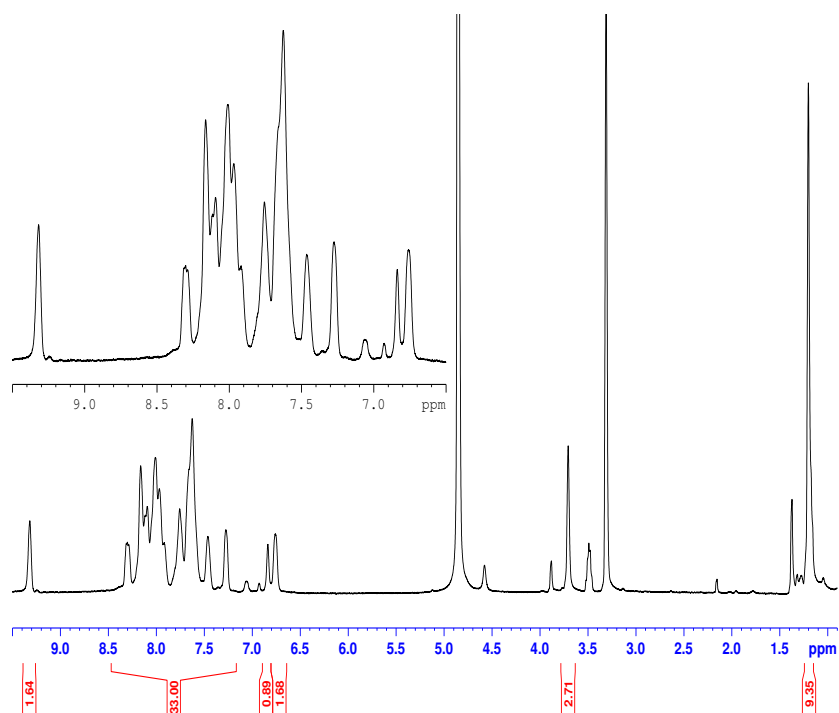


**Figure S17.** <sup>1</sup>H NMR of compound **3** in CD<sub>3</sub>OD. Note that compounds containing the bps ligand are known to give very poor quality NMR data.

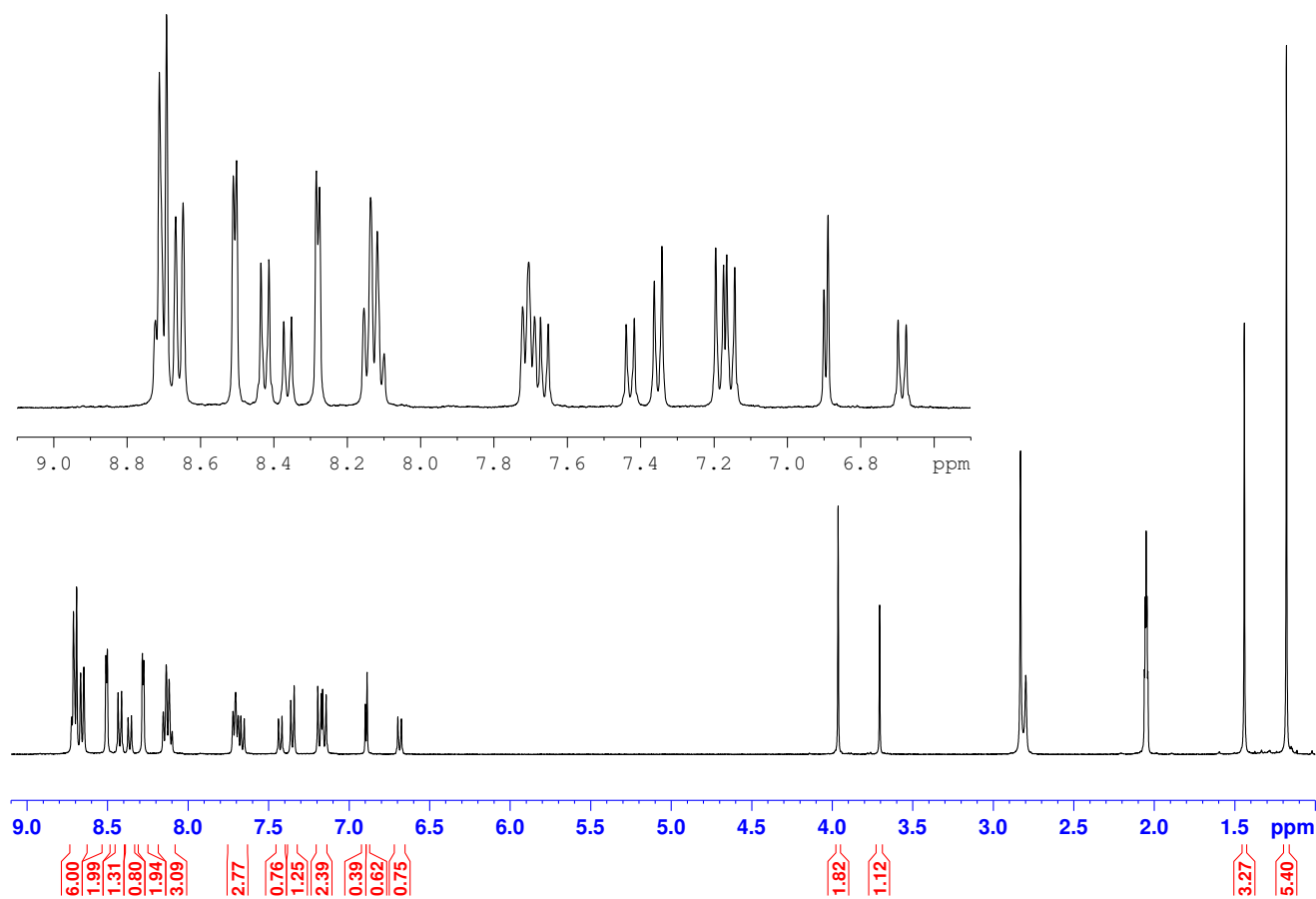


**Figure S18.**  $^1\text{H}$  NMR of compound **4** in acetone- $\text{d}_6$ .



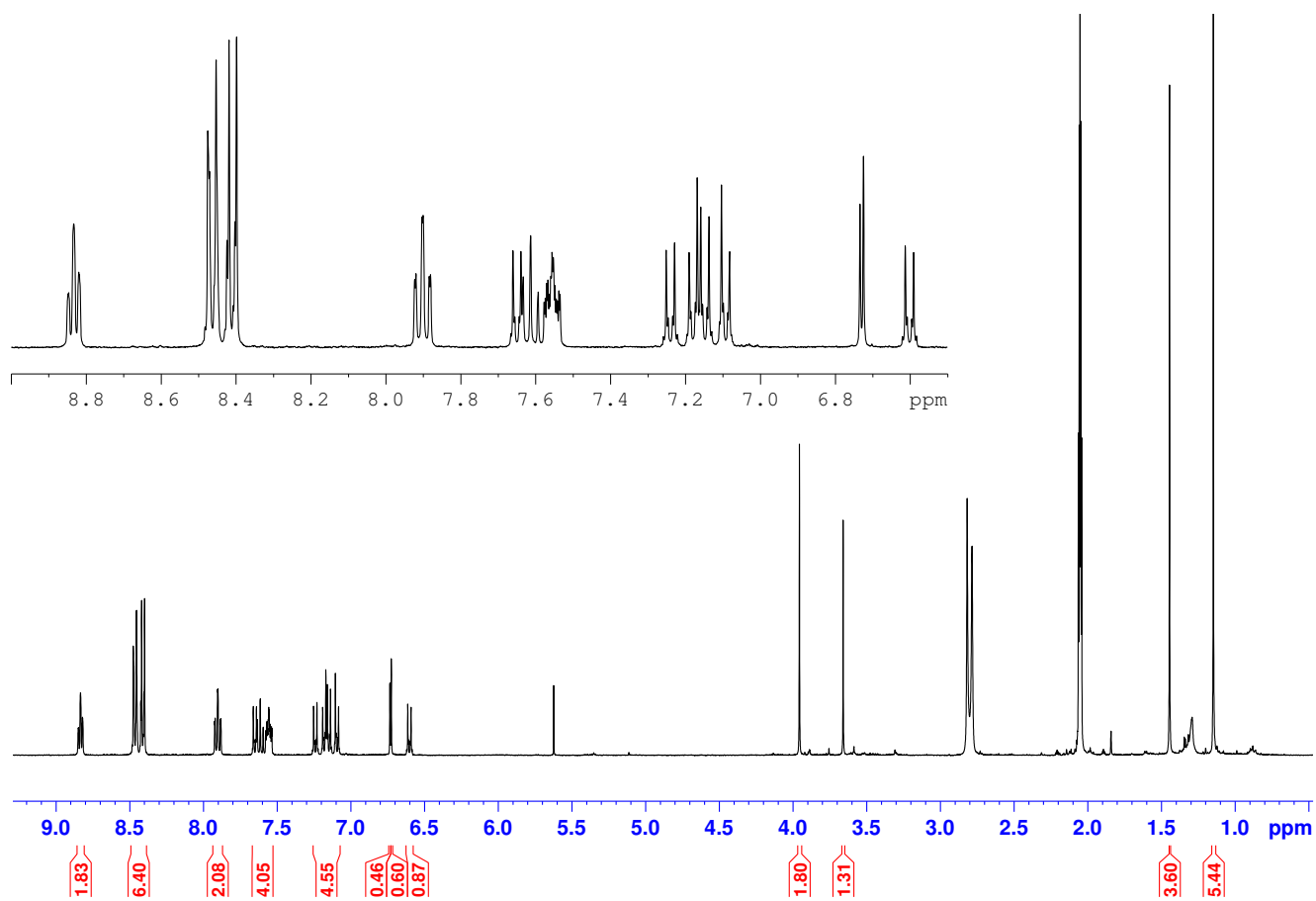


**Figure S19.** <sup>1</sup>H NMR of compound **5** in acetone-d<sub>6</sub>.

SpinWorks 4:

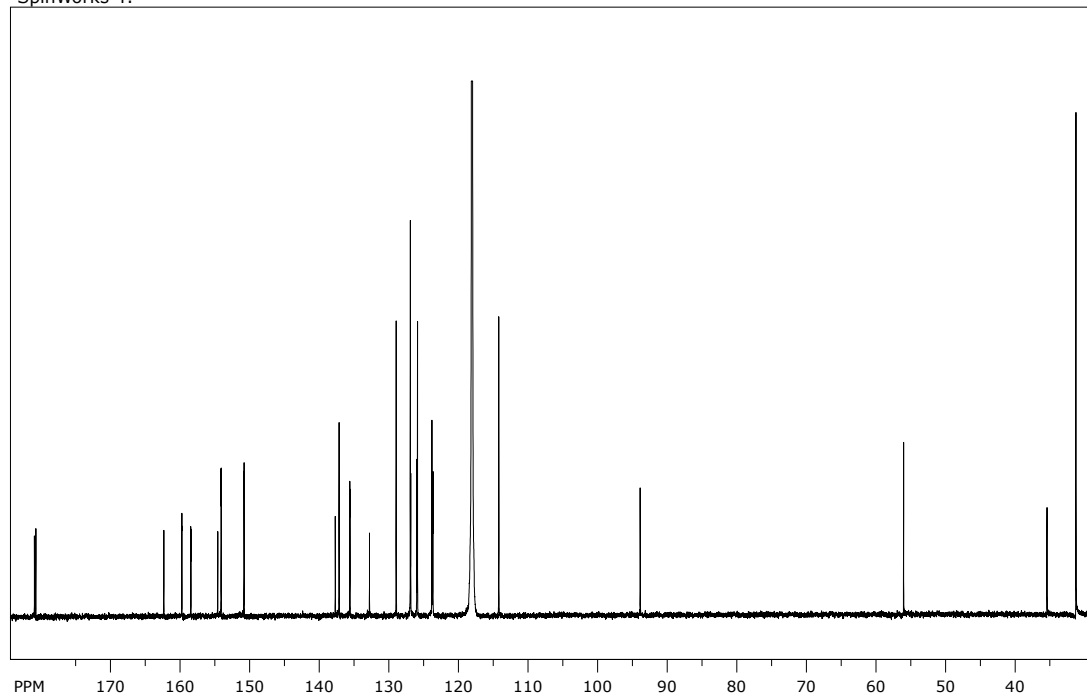


**Figure S20.** <sup>13</sup>C NMR of compound **1** in CD<sub>3</sub>CN.

SpinWorks 4:

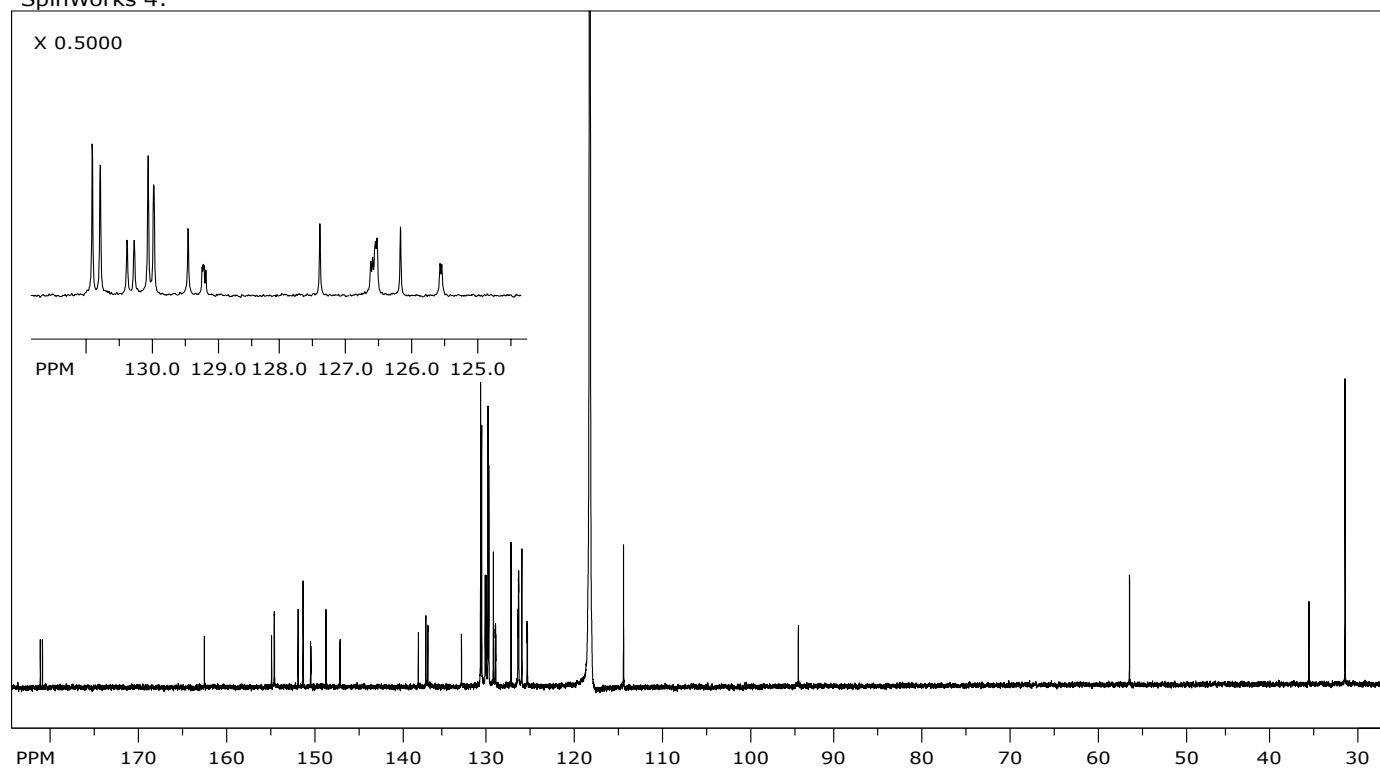


**Figure S21.** <sup>13</sup>C NMR of compound **2** in CD<sub>3</sub>CN.

SpinWorks 4:

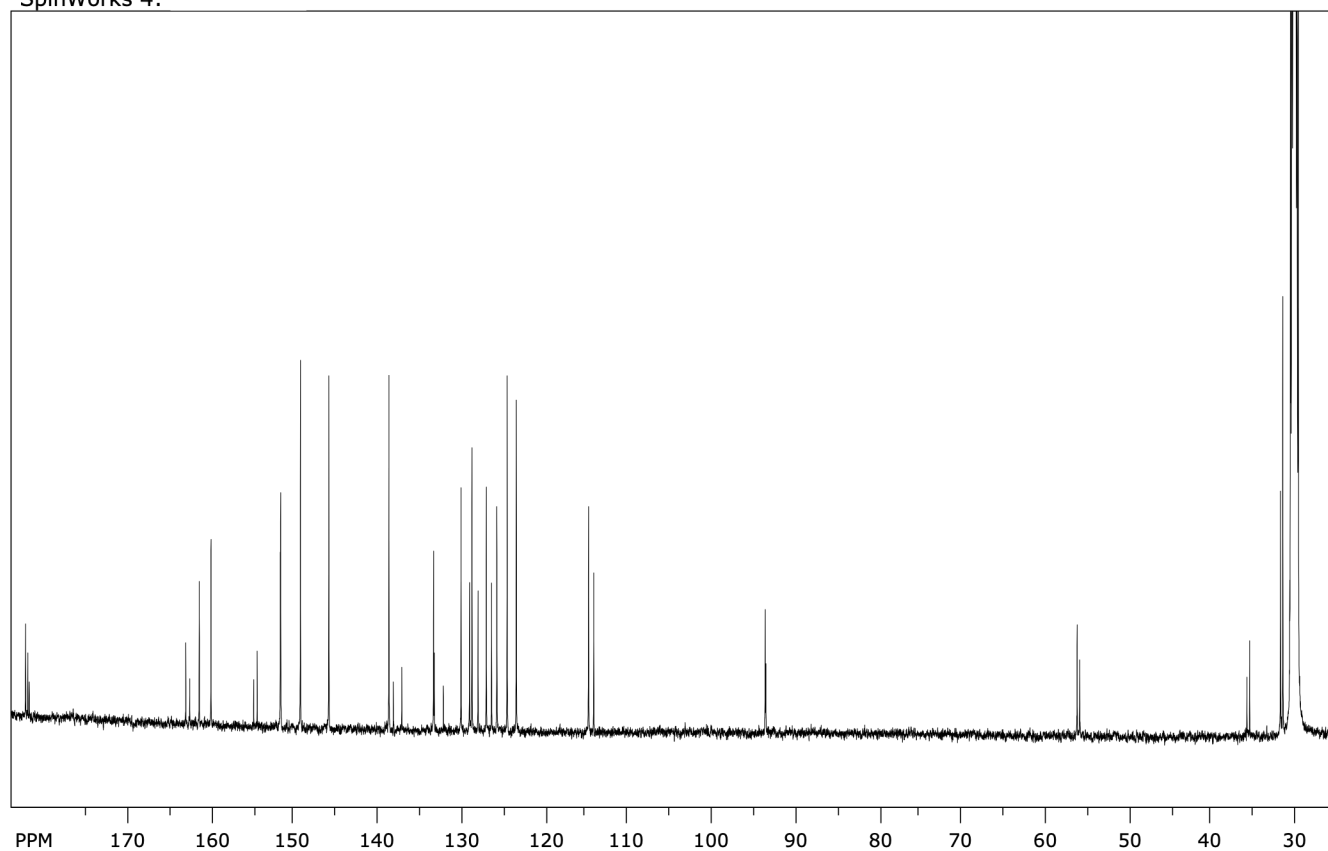


**Figure S22.**  $^{13}\text{C}$  NMR of **4** in acetone- $\text{d}_6$ . This is a mixture of isomers with duplication of signals due to the asymmetry of the AVB ligand.

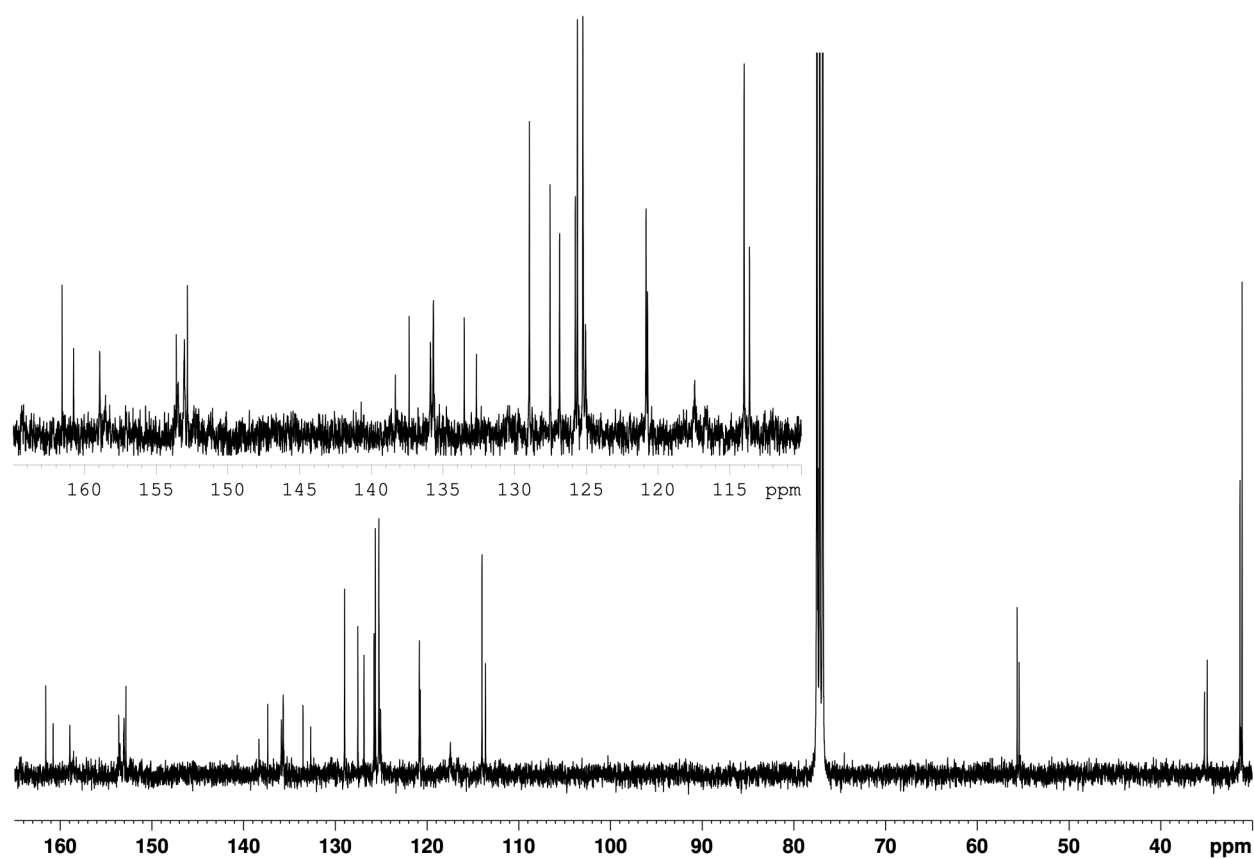


**Figure S23.**  $^{13}\text{C}$  NMR of **5** in  $\text{CDCl}_3$ . This is a mixture of isomers with duplication of signals due to the asymmetry of the AVB ligand.

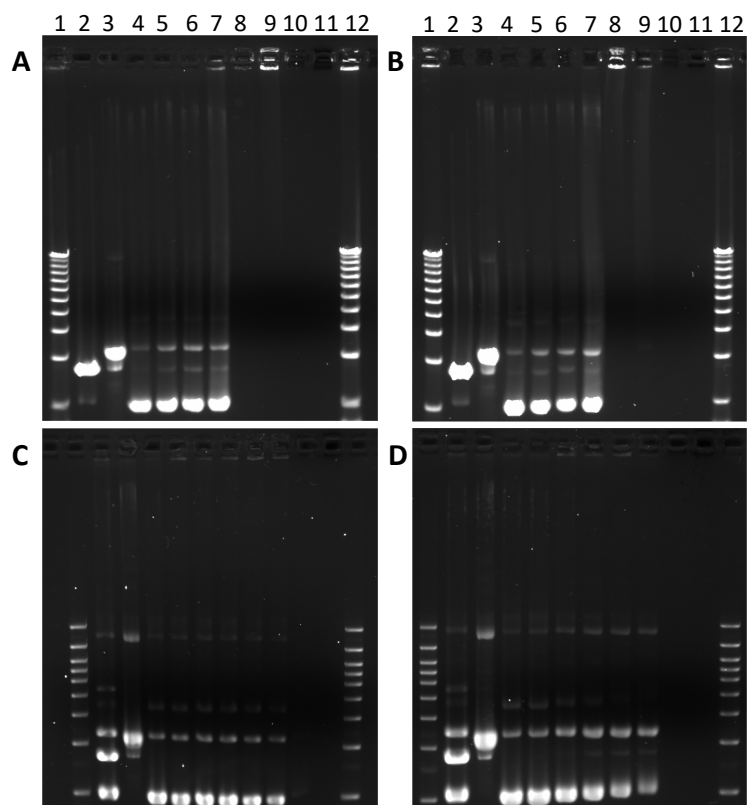


**Figure S24.** Agarose gel electrophoresis of pUC19 plasmid ( $40 \mu\text{g mL}^{-1}$ ; 10 mM phosphate buffer, pH 7.4) showing presence or absence of DNA in the wells. (A) Compound **1** without light activation, (B) with light activation ( 470 nm,  $37 \text{ J}\cdot\text{cm}^{-2}$ ), (C) compound **2** without light activation, (D) with light activation ( 470 nm,  $37 \text{ J}\cdot\text{cm}^{-2}$ ). Lanes 1 and 12, DNA molecular weight standard; lane 2, linear pUC19; lane 3, relaxed circle [Cu(phen)<sub>2</sub> reaction with pUC19]; lanes 4–11, 0, 7.8, 15.6, 31.25, 62.5, 125, 250, and 500  $\mu\text{M}$  compound.

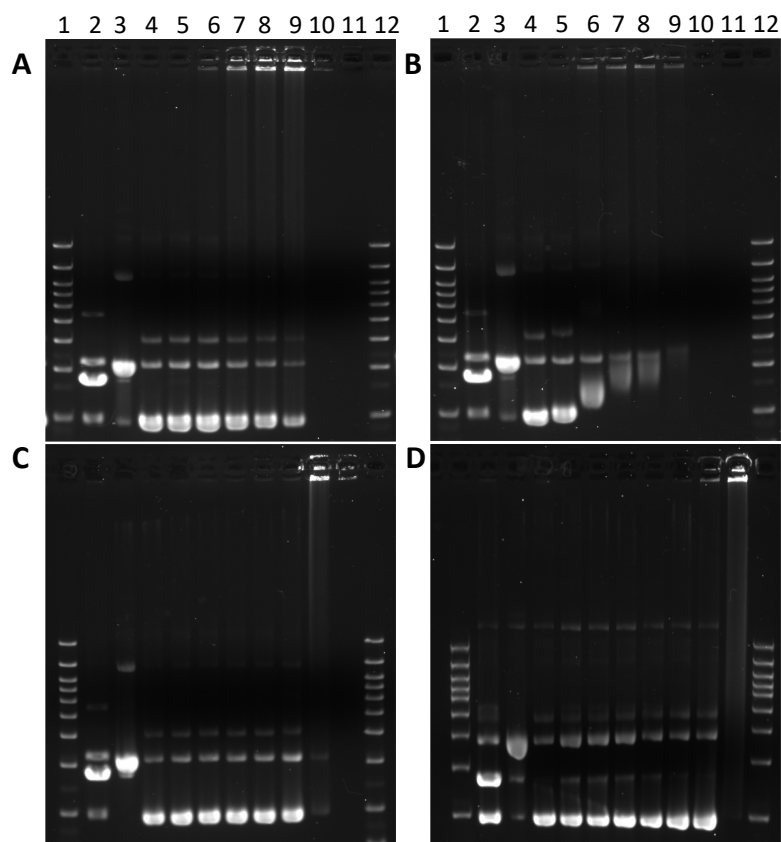


**Figure S25.** Agarose gel electrophoresis of pUC19 plasmid ( $40 \mu\text{g mL}^{-1}$ ; 10 mM phosphate buffer, pH 7.4) showing presence or absence of DNA in the wells. (A) Compound **4** without light activation, (B) with light activation ( 470 nm,  $37 \text{ J}\cdot\text{cm}^{-2}$ ), (C) compound **6** (D) compound **7**. Lanes 1 and 12, DNA molecular weight standard; lane 2, linear pUC19; lane 3, relaxed circle  $[\text{Cu}(\text{phen})_2]$  reaction with pUC19; lanes 4–11, 0, 7.8, 15.6, 31.25, 62.5, 125, 250, and 500  $\mu\text{M}$  compound.

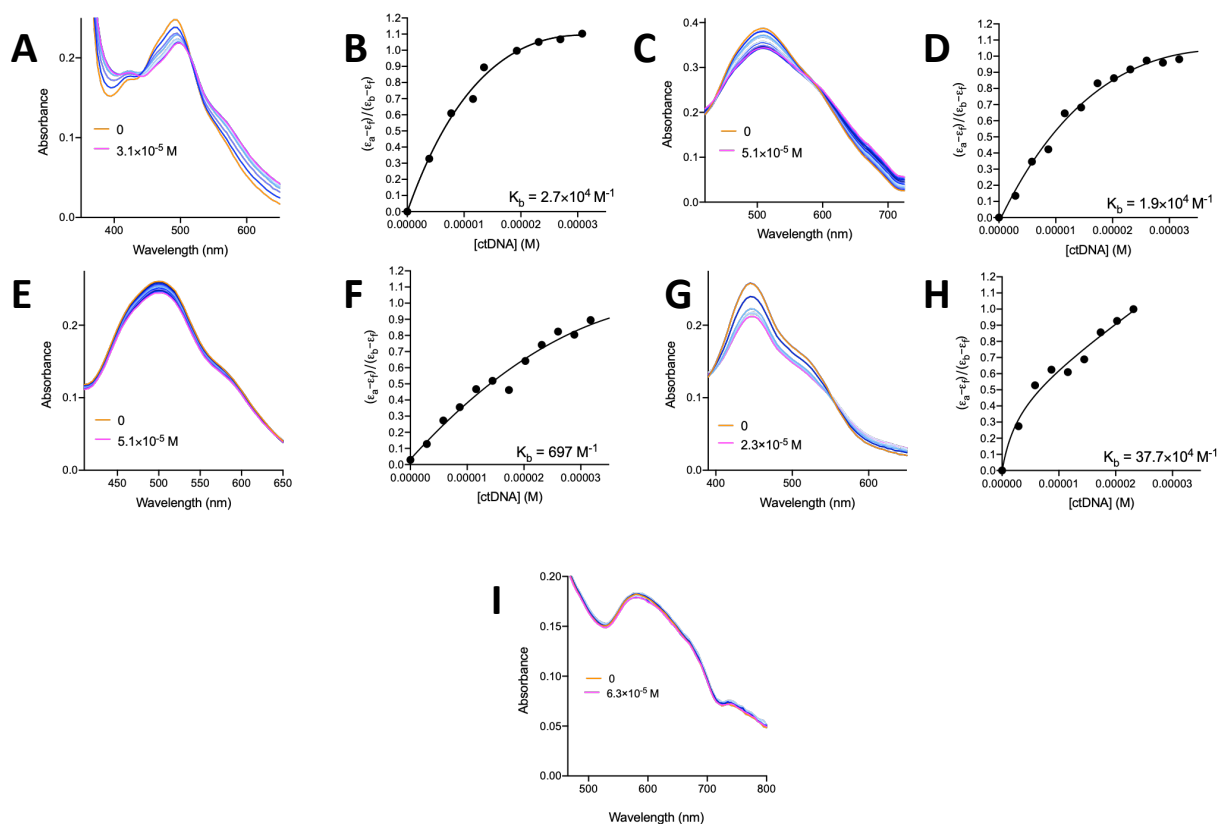


**Figure S26.** Calf thymus DNA titration monitored by UV/Vis and plots of  $(\epsilon_a - \epsilon_f)/(\epsilon_b - \epsilon_f)$  vs ctDNA concentration.  $\epsilon_a$  is the apparent absorption of the complex in the presence of DNA,  $\epsilon_b$  is the attenuation coefficient of the DNA-bound Ru complex, and  $\epsilon_f$  is the attenuation coefficient of the unbound complex in buffer. Compound **1** (A and B), **2** (C and D), **3** (E and F), **4** (G and H), and **5** (I) in phosphate buffer (50 mM, pH = 7.4). Complex **5** did not show changes under our conditions.

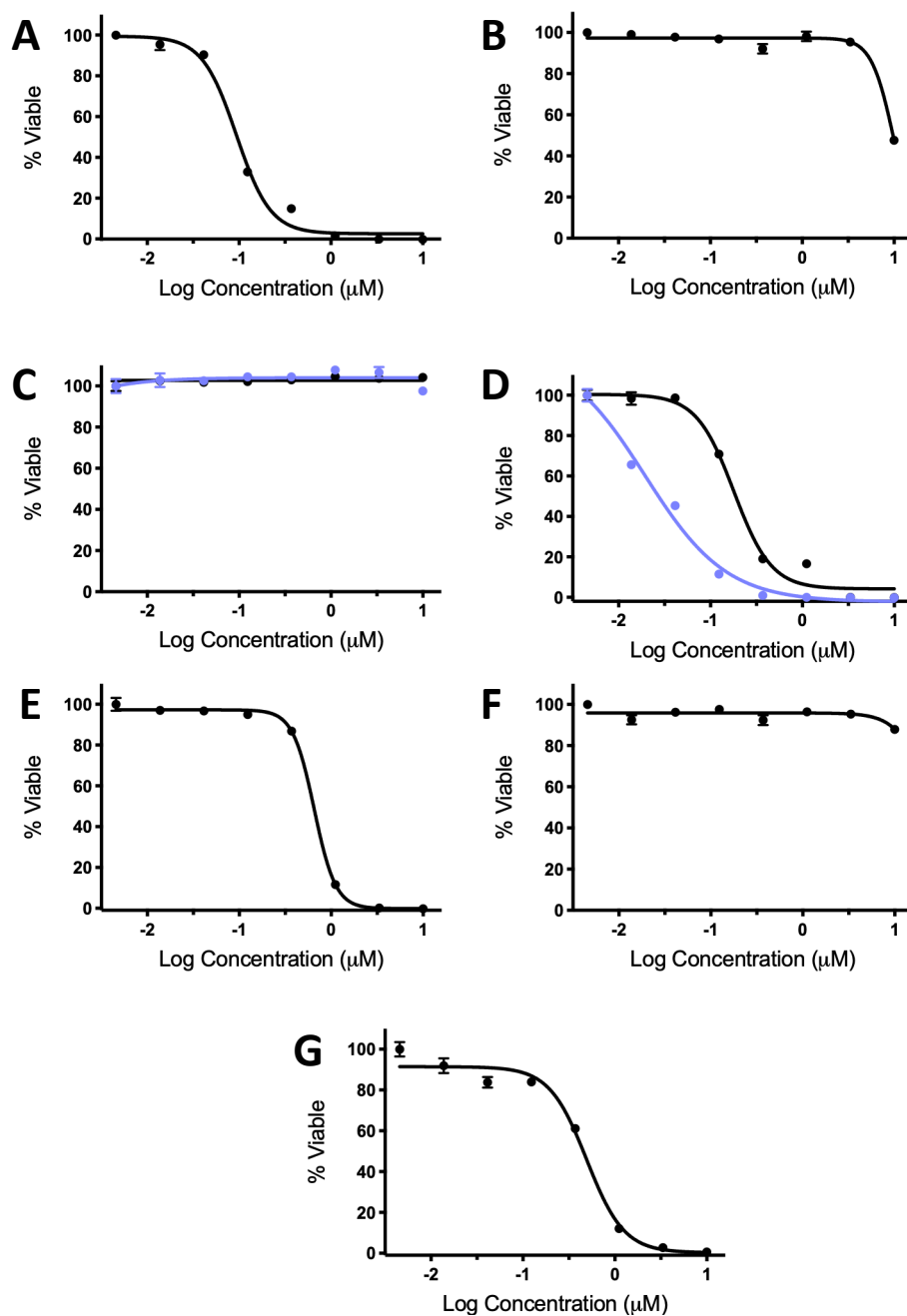


**Figure S27.** Cytotoxicity dose responses for **1** (A), **2** (B), **3** (C), **4** (D), **5** (E), **6** (F), **7** (G) in DU145 cells. Compounds **1–7** under dark conditions (black), and compounds **3** and **4** under light conditions (Indigo light  $>450$  nm  $29.1$  J/cm $^2$  for 60 s, blue line).



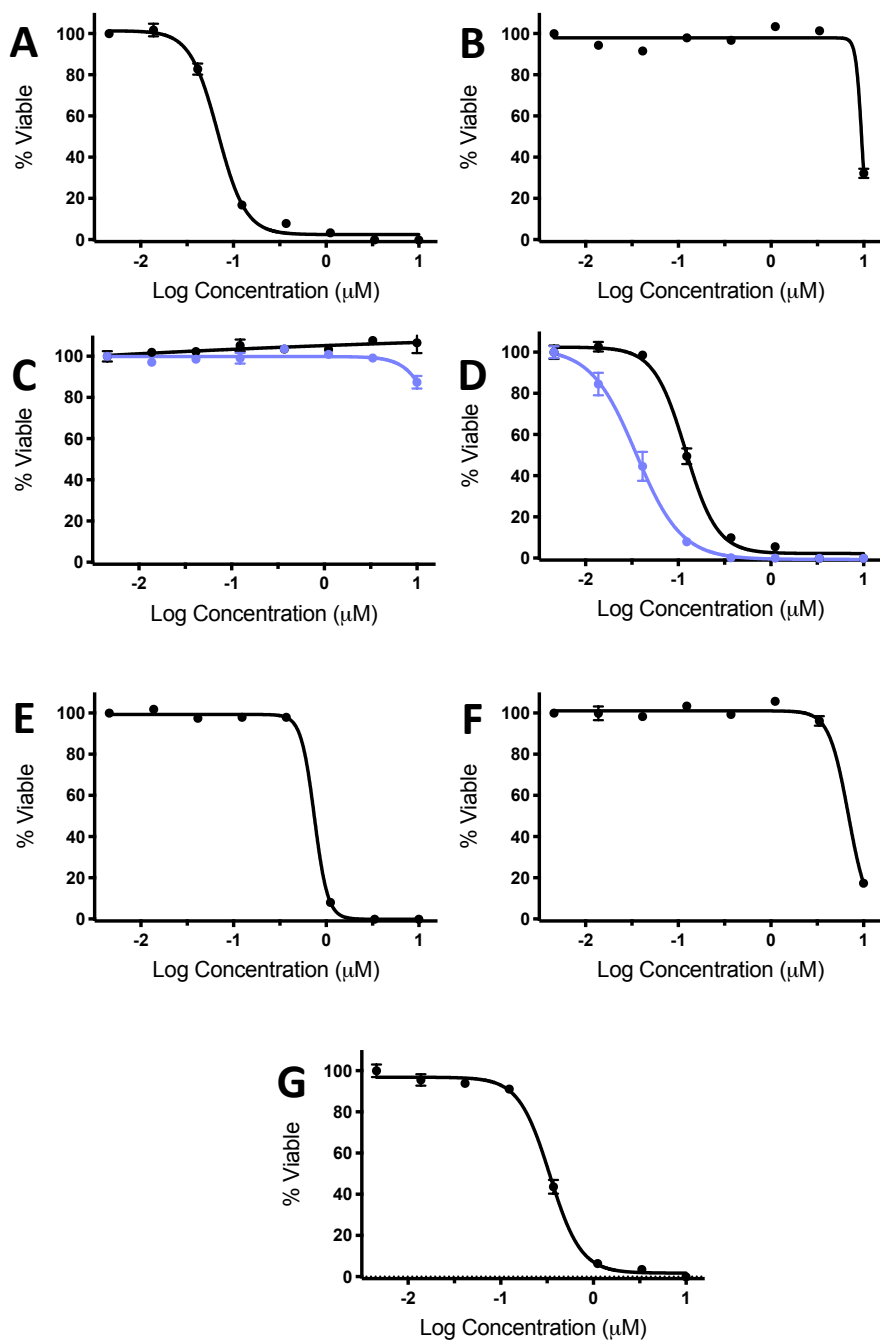


**Figure S28.** Cytotoxicity dose responses for **1** (A), **2** (B), **3** (C), **4** (D), **5** (E), **6** (F), **7** (G) in MIA PaCa-2s cells. Compounds **1–7** under dark conditions (black), and compounds **3** and **4** under light conditions (Indigo light  $>450\text{ nm}$   $29.1\text{ J/cm}^2$  for 60 s, blue line).

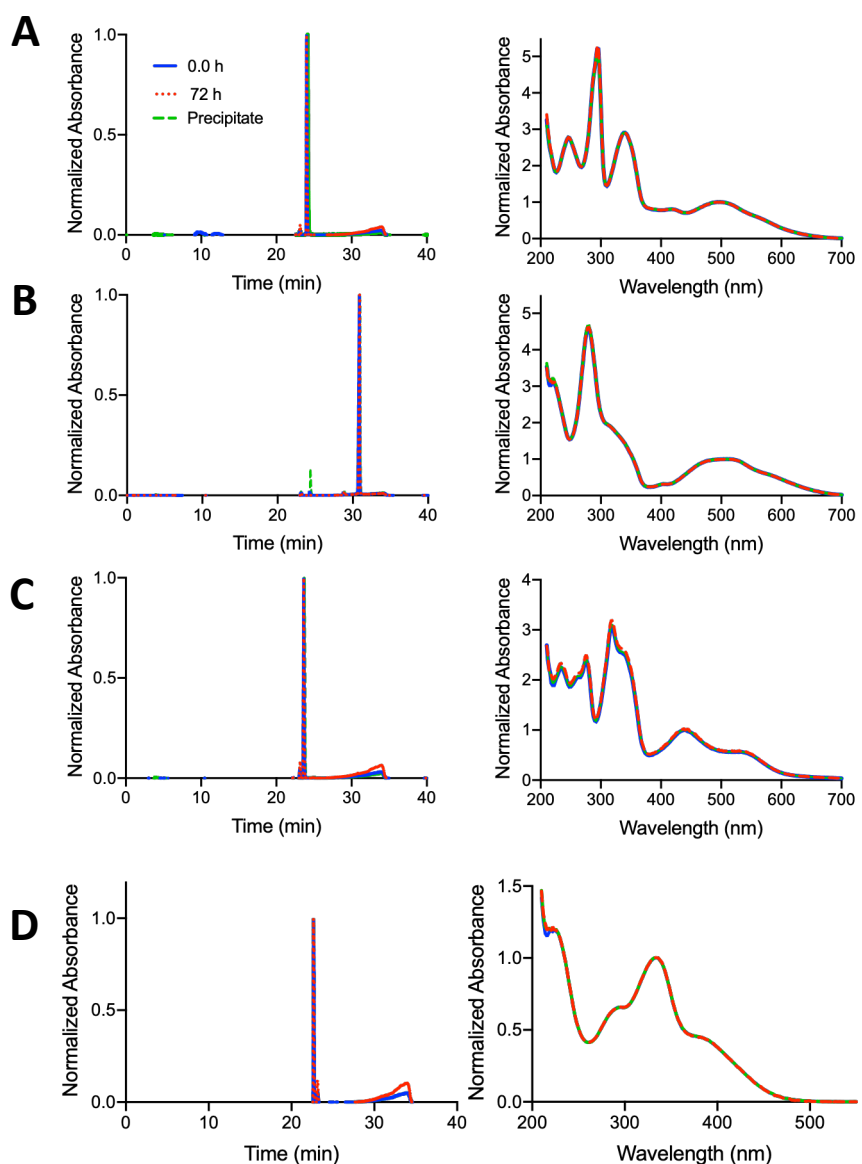


**Figure S29.** Compound stability measured by HPLC (left) before (blue) and after (red) 72 h incubation in water for **1** (A), **2** (B), **4** (C), **7** (D). A small amount of precipitate that formed over the course of 72h and was redissolved and measured (green line). A slight (< 0.6%) variation of retention time was seen for some compounds and the identity was confirmed by absorbance spectra (right). The broad peak at 30-35 min is present in the blank spectrum.

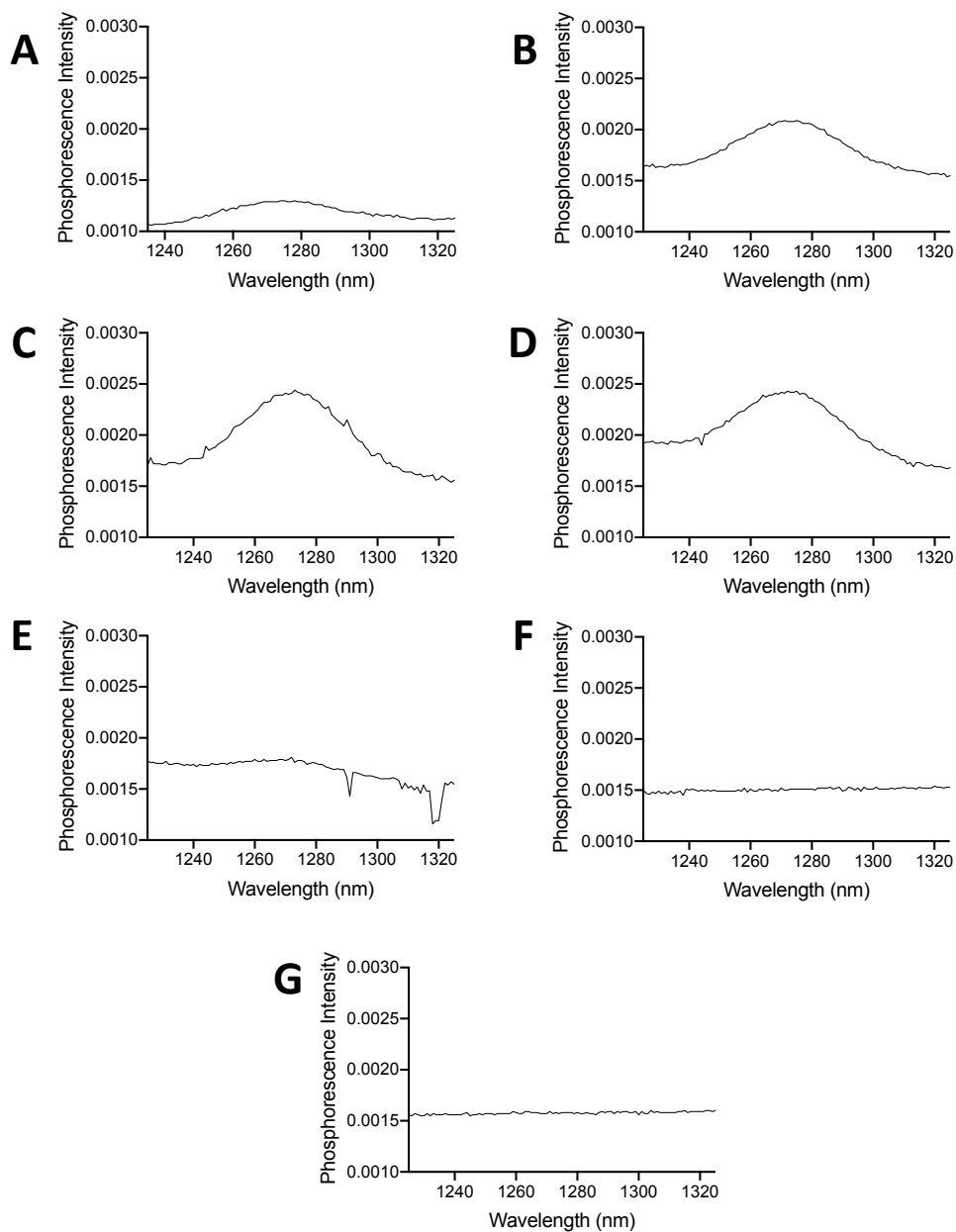


**Figure S30.** Detection of singlet oxygen production from **1** (A), **2** (B), **3** (C), **4** (D), **5** (E), **6** (F), **7** (G) in CD<sub>3</sub>OD. Samples were measured as isoabsorptive solutions with absorbance  $\sim 0.2$ . The peak at 1275 nm corresponds to the phosphorescence from singlet oxygen.

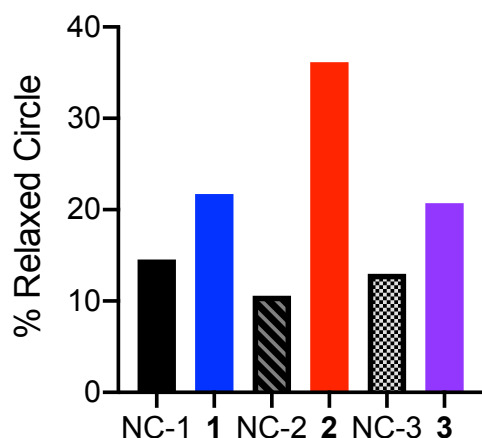


**Figure S31.** Quantification of relaxed circle DNA for **1**, (blue) **2** (red) and **3** (purple) relative to a no compound control (NC, black bars) for each experiment. The corresponding gels can be found in Fig 2 B and D and Fig. S5B.

### 13. References

1. R. Pettinari, F. Marchetti, A. Petrini, C. Pettinari, G. Lupidi, P. Smoleński, R. Scopelliti, T. Riedel and P. J. Dyson, *Organometallics*, 2016, **35**, 3734-3742.
2. H. Audi, D. F. Azar, F. Mahjoub, S. Farhat, Z. El Masri, M. El-Sibai, R. J. Abi-Habib and R. S. Khnayzer, *J. Photochem. Photobiol., A*, 2018, **351**, 59-68.
3. M. M. McGoorty, R. S. Khnayzer and F. N. Castellano, *Chem Commun*, 2016, **52**, 7846-7849.
4. M. M. McGoorty, A. Singh, T. A. Deaton, B. Peterson, C. M. Taliaferro, Y. G. Yingling and F. N. Castellano, *ACS Omega*, 2018, **3**, 14027-14038.
5. D. K. Heidary, B. S. Howerton and E. C. Glazer, *J. Med. Chem.*, 2014, **57**, 8936-8946.
6. D. Havrylyuk, M. Deshpande, S. Parkin and E. C. Glazer, *Chem. Commun.*, 2018, **54**, 12487-12490.
7. S. R. Dalton, S. Glazier, B. Leung, S. Win, C. Megatuluski and S. J. N. Burgmayer, *J. Biol. Inorg. Chem.*, 2008, **13**, 1133.
8. M. G. Haney, L. H. Moore and J. S. Blackburn, *J Vis Exp*, 2020, DOI: 10.3791/60996.